98P

UNPUBLISHED PRELIMINARY DATA

FACILITY FORM 602
N64-29504
(ACCESSION NUMBER)
92
(PAGES)
CR-58346
(NASA CR OR TMX OR AD NUMBER)
(THRU)
1
(CODE)
29
(CATEGORY)

INVESTIGATIONS OF THE TEMPERATURE AND SPECTRAL EMISSIVITY CHARACTERISTICS OF CLOUD TOPS AND OF THE EARTH'S SURFACE

First Semiannual Progress Report

by

William E. Marlatt

A progress report conducted under Contract NASr-147 between the National Aeronautics and Space Administration and Colorado State University.

Technical Paper No. 51
Department of Atmospheric Science
Colorado State University
Fort Collins, Colorado

February 1964

OTS PRICE
XEROX $ 8.60 ph
MICROFILM $

REPORTS CONTROL No.

INVESTIGATIONS OF THE TEMPERATURE AND SPECTRAL EMISSIVITY CHARACTERISTICS OF CLOUD TOPS AND OF THE EARTH'S SURFACE

First Semiannual Progress Report

by

William E Marlatt

A progress report conducted under Contract NASr-147 between the National Aeronautics and Space Administration and Colorado State University.

Technical Paper No. 51
Department of Atmospheric Science
Colorado State University
Fort Collins, Colorado

February 1964

TABLE OF CONTENTS

Summary. 1

Objective I. 1

Objective II 49

Objective III 57

Objective IV 57

Bibliography. 59

Acknowledgment. 60

Appendix A. . . . . A. 1-8

Appendix B. . . . . B. 1-20

SUMMARY

29504

In May, 1963, the Department of Atmospheric Science of Colorado State University began an investigation of certain aspects of infrared radiation transfer through the earth's atmosphere under NASA contract number NASr-147. The basic objectives of the study were: (1) to investigate the relationship between actual earth surface temperature and the temperature of cloud tops and the observed temperatures of these surfaces as measured by radiometers aboard aircraft and meteorological satellites, (2) to provide ground and low level aircraft support for field studies conducted by the National Aeronautics and Space Administration, (3) to investigate the relationship between cloud top radiation and the air temperature outside the cloud at cloud top height, (4) to investigate the spectral emissivity characteristics of (a) various cloud types and (b) the surface of the earth in desert, grassland, and forested regions.

During the period covered by this progress report (May 1963 - February 1964) primary emphasis has been placed on objectives one and two.

Author

OBJECTIVE 1

Introduction

The initial emphasis of this objective has been an investigation of the relationship between actual temperatures of the surface of the earth and the black body temperature as measured by a radiometer mounted on the underside of a Cessna 180 aircraft, and by channel 2 (8-13 micron band) of TIROS VII. Basically this objective stems from the need for a better understanding of the transmission losses in the "window" region of the spectrum of the terrestrial radiation passing through the earth's atmosphere.

Several researchers (Bandeen, et. al., 1961; Fritz and Winston, 1962; Hanel and Stroud, 1961) have used channel 2 measurements from TIROS satellites to estimate surface temperatures of the earth under

clear skies. These estimated surface temperatures were invariably several degrees too low. Wark, et. al. (1962) has shown that, even though the absorption coefficients of water vapor and ozone are relatively small in the window region, certain corrections in the satellite measurement of outgoing terrestrial radiation intensity are necessary to account for the influence of these two atmospheric consitutents. In each of the studies reported, however, no exact values of the earth's surface temperature were known.

In the investigation discussed in this report, an attempt was made to obtain accurate measurements of actual earth surface temperatures in an area of nearly uniform vegetation and terrain. Surface temperature measurements were made during different seasons and at various times of the day and night, each observation time corresponding to the time of an overpass of TIROS VII. Concurrent with each overpass, a profile of outgoing radiation measurements were recorded from the earth surface to airplane ceiling height (approximately 17,000 - 19,000 feet m. s. l.). The radiometer used for these measurements was the infrared radiometer, model IT-2, manufactured by the Barnes Instrument Co.

Radiation data from channel 2 of TIROS VII meteorological satellite are currently being analyzed by Dr. Fujita of the University of Chicago. This report will discuss only the measurements made at the earth surface and from the airplane.

Site Requirements and Method of Measurements

Measurement of the earth surface temperatures: Emphasis to date has been placed on collection of accurate temperature measurements over a region of relatively uniform vegetation within the Pawnee National Grassland of Northeastern Colorado. Vegetation within the grassland region consists, for the most part, of short native buffalo and grama grasses. A few, small scattered acreages within the national grassland are under cultivation, mostly to winter wheat. Only small differences in outgoing radiation are noted between the wheat fields and adjacent pasturelands during most seasons. Fig. 1 shows the location of the Pawnee National Grassland. Fig. 2 shows a general view of the research site.

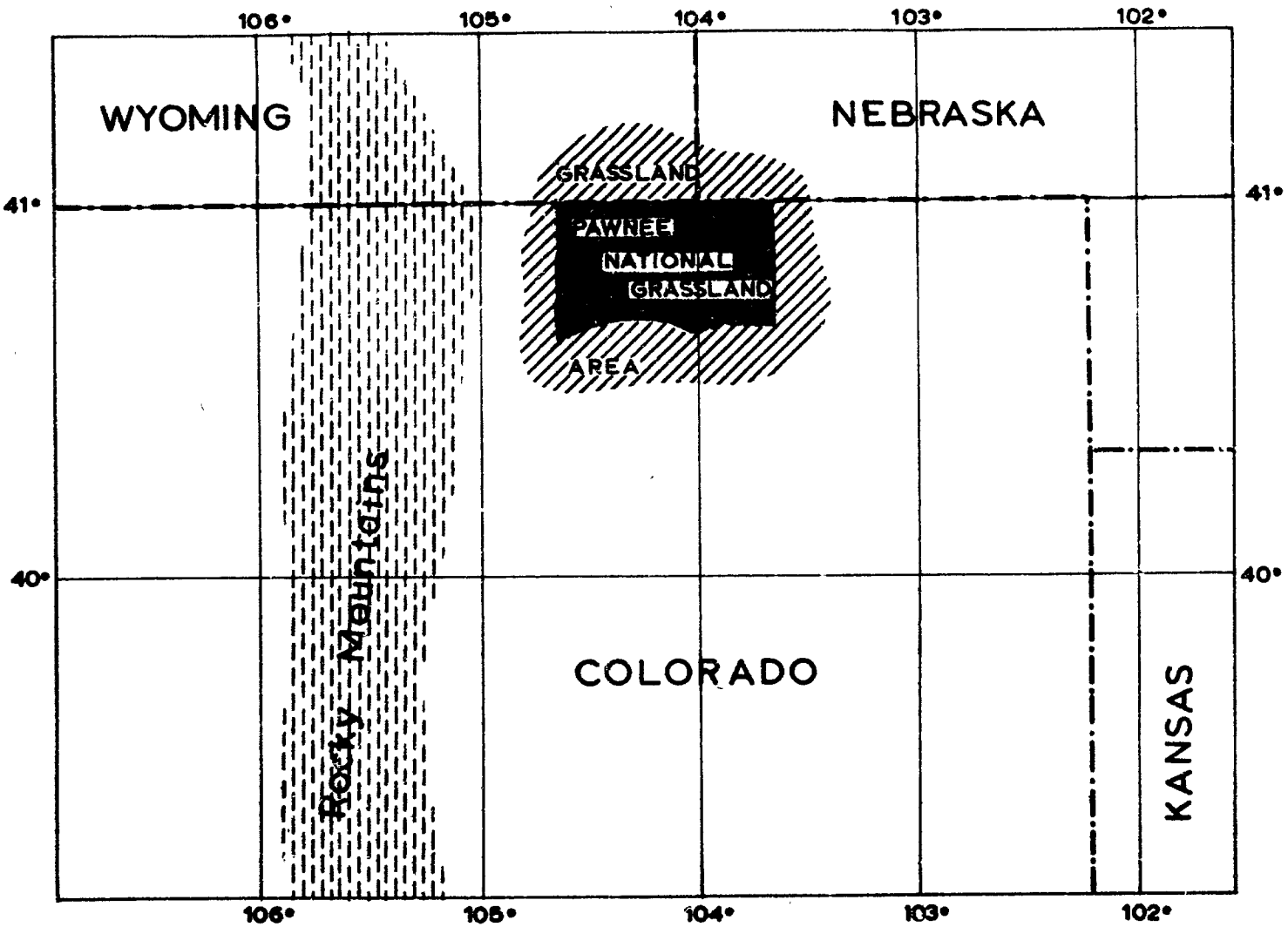

Fig. 1 Map of grassland region used in NASA radiation field study. Pawnee National Grassland area is double hatched; regional grassland area is hatched.

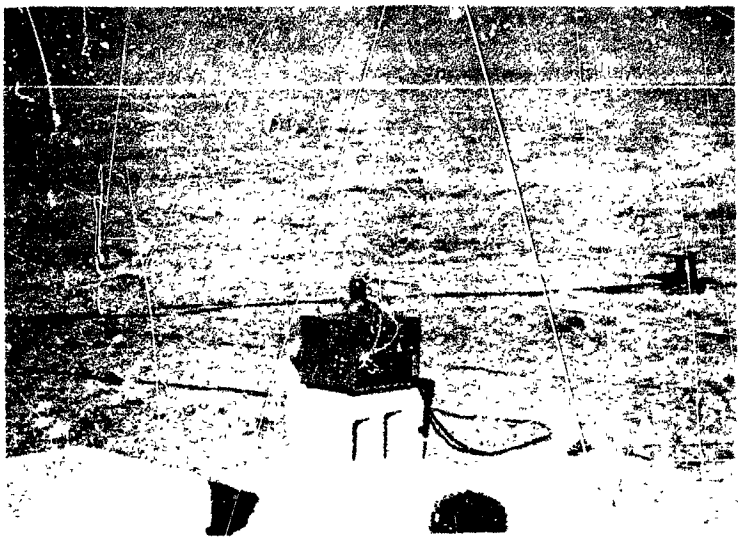

Fig. 2 General view looking north across surface temperature measurement site. Pawnee National Grassland, Colorado.

Instrumentation for measurement of surface temperatures has been installed near the geographical center of the national grassland approximately fifteen miles west of Grover, Colorado. Twenty-eight sensors were used in the first installation network. The sensors consisted of small electronic stabistors spread over a circle of 100 foot radius. Changes in the temperature of the stabistor produced a linear change in its resistance and was recorded by a wheatstone bridge circuit. Due to damage by rodents, this unit was replaced in November 1963 by a second model which employed forty thermistor sensors spread over an area of 1,000 foot radius. Simultaneous measurements using both units indicated midday temperature differences of less than 0.3° C.

The true temperature of the surface of the earth is, at best, an extremely nebulous value. This is due primarily to the extremely steep gradients of temperature(both in the horizontal and in the vertical) that frequently exist in this zone. A perfect sensor for measuring

the true surface temperature would have to be infinitely thin and possess thermal and moisture properties identical to those of the soil particles themselves. The presence of grass or other vegetation is a further compounding factor in the measurement of earth surface temperatures. Fig. 3 shows the distribution of temperatures in and around a small clump of buffalo grass at 0900 on January 21, 1964. The temperature distribution shown in this figure are given as an example of the steepness of the temperature gradients in the microlayer and indicate the difficulty of positioning sensors for determining true averages of surface temperature. Temperatures shown in this figure were obtained by using a portable thermistor probe.

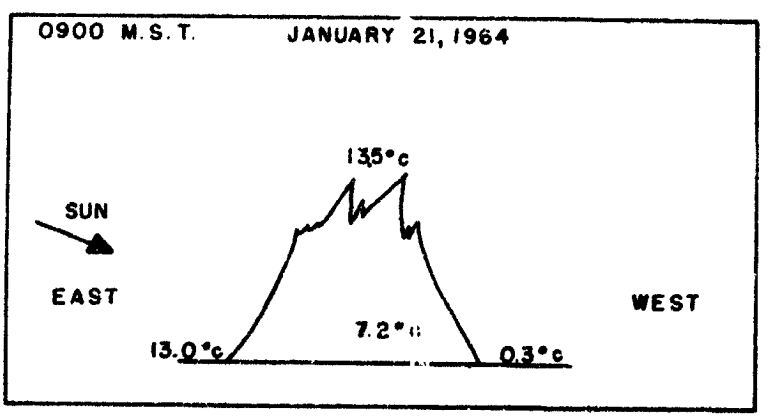

Fig. 3 Distribution of surface temperature in and around a buffalo grass clump 0900 MST, January 21, 1964.

To overcome, at least in part, the above described difficulties, the sensors used were: (1) physically as small as practical, (2) painted

the same color as the soil surface (light grey), and (3) coated while the paint was still wet with one layer of dust. Fig. 4 shows a comparison of size of the two sensors used.

Fig. 4 Comparison of size of bead thermistor and stabistor units used for surface temperature measurements.

The sensors were placed randomly over the site area. Some were located inside grass clumps, others on the bare ground between clumps. The stabistor sensors which were placed on the bare ground were pressed halfway into the soil so that they measured the integrated temperature across the zone from $1\frac{1}{2}$ mm above to $1\frac{1}{2}$ mm below the soil surface. The bead thermistors which replaced the stabistors are less than 1 mm thick and were installed flush with the soil surface. Positioning of the sensors is checked prior to each measurement.

Fig. 5 "Tent" shields used to eliminate radiation heating of the stabistor units.

To prevent erroneous temperature measurements due to radiation heating of the sensors during observation periods with strong sunshine, "tent" shields (fig. 5), made from louvered aluminum screen were placed over the stabistor units a few minutes before observation time. Measurements with and without the shields indicated insignificant temperature differences for the thermistor beads. No shields are used over the thermistor bead units.

Recording of surface temperature measurements from the network of sensors required approximately fifteen minutes for the stabistor unit and five minutes for the thermistor unit. Two sets of measurements are averages for each TIROS VII satellite overpass flight.

Changes in earth surface temperature within the recording period are always much smaller than the difference between measurement points. Table 1 shows a sample of average surface temperatures with their

standard deviations for different times of the day and night. Table 1 also shows a comparison of average temperatures as measured by the thermistor units to average black body temperature measured by the 3° view, 8-13 micron filter radiometer held approximately twelve inches above the thermistor units.

The effect of emissivity on the comparison of actual temperature to black body radiation temperature needs much further investigation. A pilot, laboratory study on the emissivity of grassland soils is given in Appendix A.

Air temperatures and relative humidities are measured by a sling psychrometer.

TABLE 1. Actual and Black Body Temperatures.
Pawnee National Grassland, February 10 and 11, 1964.

		Actual		Radiation	
Date	MST Time	Surface Temp. °C	Standard Deviation °C	Black Body Temp. °C	Standard Deviation °C
2/10/64	1100	17.2	3.6	17.0	3.2
	1300	23.4	3.2	21.4	3.2
	1500	13.6	3.3	17.1	3.4
	1935	- 4.8	1.5	- 2.8	1.3
	2130	- 3.8	1.1	- 3.2	1.3
	2330	- 7.5	1.3	- 5.8	0.9
2/11/64	0130	- 7.1	1.0	- 5.3	2.5
	0330	- 7.5	0.8	- 5.1	0.3
	0540	- 4.4	0.7	- 3.8	1.0
	0735	- 2.4	1.0	- 3.2	0.7
	0945	8.4	1.7	7.2	1.7
	1150	12.0	1.3	11.9	0.8

Aircraft radiation measurements: Airborne measurements of terrestrial radiation are obtained using the IT-2 infrared radiometer (Barnes Instrument Co.) mounted on a Cessna 130 airplane. The IT-2 radiometer employs an indium antimonide AR coated filter system which is transparent across the 8 to 13 micron region of the electromagnetic spectrum. Transmission curves supplied by the Barnes Instrument Co. indicate that the transmission of this filter may extend well beyond 13 microns. Independent spectral calibration of the total instrument is planned.

The view angle of the radiometers used in the satellite overpass flights is approximately 30°. Table 2 shows the relation between view area and height. Figs. 3 through 11, taken at increasing altitudes above the grassland site show the area viewed by the radiometer.

TABLE 2. Area Viewed by the IT-2, 30° Radiometer at Various Heights

Height above surface	Diameter of area viewed
1,000	268
2,000	533
3,000	803
4,000	1072
6,000	1607
8,000	2143
10,000	2679
12,000	3215
14,000	3751
16,000	4287

Response time of the radiometer is adjustable for either 50 or 500 milliseconds, the later being used on most flights to conform to the response time of the recorder used and also to reduce background "noise" caused by small areas of non-representative surface temperatures.

Fig. 6 Area viewed by 30° radiometer from 6,000 feet above the surface. Pawnee National Grassland.

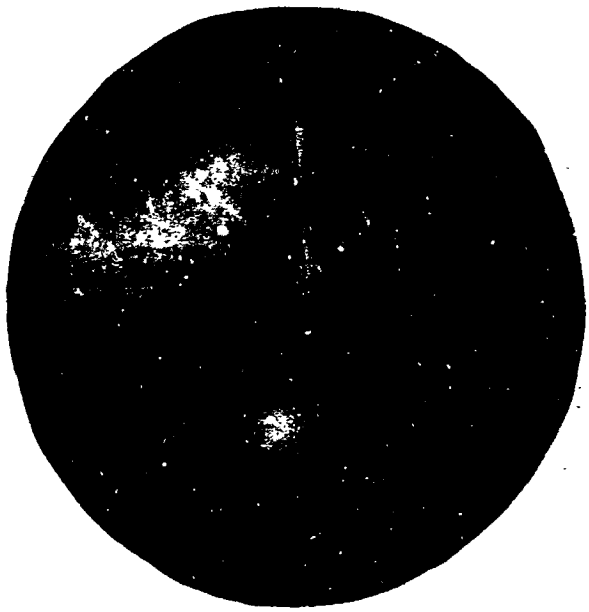

Fig. 7 Area viewed by 30° radiometer from 7,000 feet above the surface. Pawnee National Grassland.

Fig. 8 Area viewed by 30° radiometer from 8,000 feet above the surface. Pawnee National Grassland.

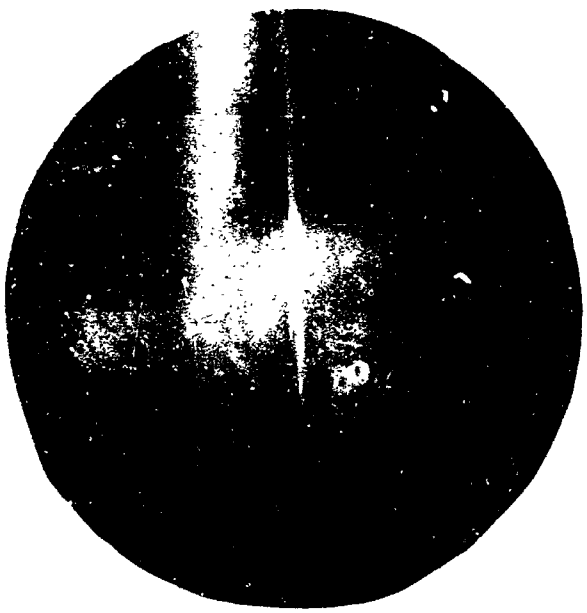

Fig. 9 Area viewed by 30° radiometer from 9,000 feet above the surface. Pawnee National Grassland.

Fig. 10 Area viewed by 30° radiometer from 10,000 feet above the surface. Pawnee National Grassland.

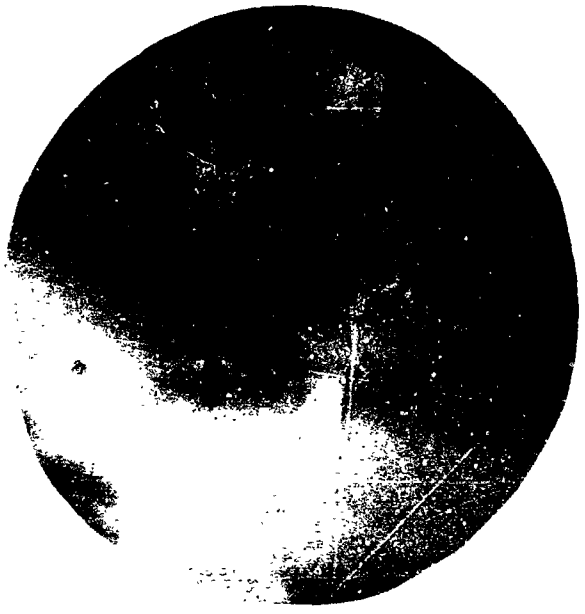

Fig. 11 Area viewed by 30° radiometer from 11,000 feet above the surface. Pawnee National Grassland.

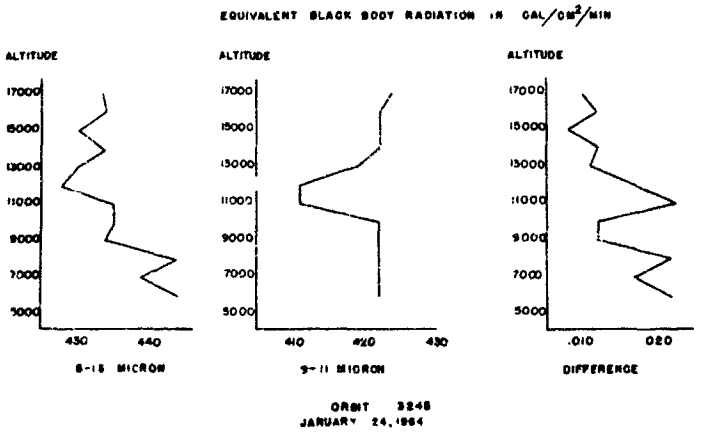

Fig. 12 Comparison of 8-13 and 9-11 micron filter radiometer for orbit 3245.

A second radiometer, identical to the first except for a narrower band filter system centered on 10.6 microns with a half-power band of 1.1 microns has been flown alongside the 8-13 micron radiometer on several flights. Fig. 12 shows a comparison of the radiation temperature from the two instruments over the Pawnee National Grassland.

A third radiometer, identical to the first except for a 3° view angle rather than the 30° view is used for special studies over grassland, desert, mountain and water areas.

Supplemental aircraft measurements: An aerograph was carried aboard the aircraft on each overpass flight. With this instrument a complete record of air temperature, relative humidity and pressure was obtained. Clock failure resulted in loss of these data for a number of flights between October 20 and November 20, 1963. Precipitable water

for use in the computations of radiation transfer were obtained for this period from radiosonde soundings from the U. S. Weather Bureau office in Denver, Colorado.

An Eppley pyrheliometer was mounted on the top of the plane and was flown on a number of flights during the autumn of 1963. Data recorded from this instrument was compared with a pyrheliometer at ground level as part of a study to quantitatively evaluate the role of atmospheric haze on radiation attenuation. A discussion of the results of these measurements is found in Appendix B.

Analysis and Discussion of Data

Figs. 13 through 43 show one-minute averages of terrestrial radiation measured by the aircraft radiometer for the TIROS VII overpasses between July, 1963 and February, 1964. Radiation in these graphs is expressed as equivalent black body temperature (°C) for comparison with surface and air temperature.

During the first fifteen to twenty minutes of the first leg of each flight, the plane flew over many types of surfaces -- farmland vegetation, small lakes, trees, etc., before reaching the grassland region. After climbing to ceiling height, the airplane flew a criss-cross pattern over a thirty mile diameter circle (corresponding to the view area of the TIROS satellite radiometer) for a short period spanning the satellite overpass time. From the third leg of each flight, a profile of radiation was measured directly above the soil temperature site from ceiling altitude down to ten feet above the earth surface.

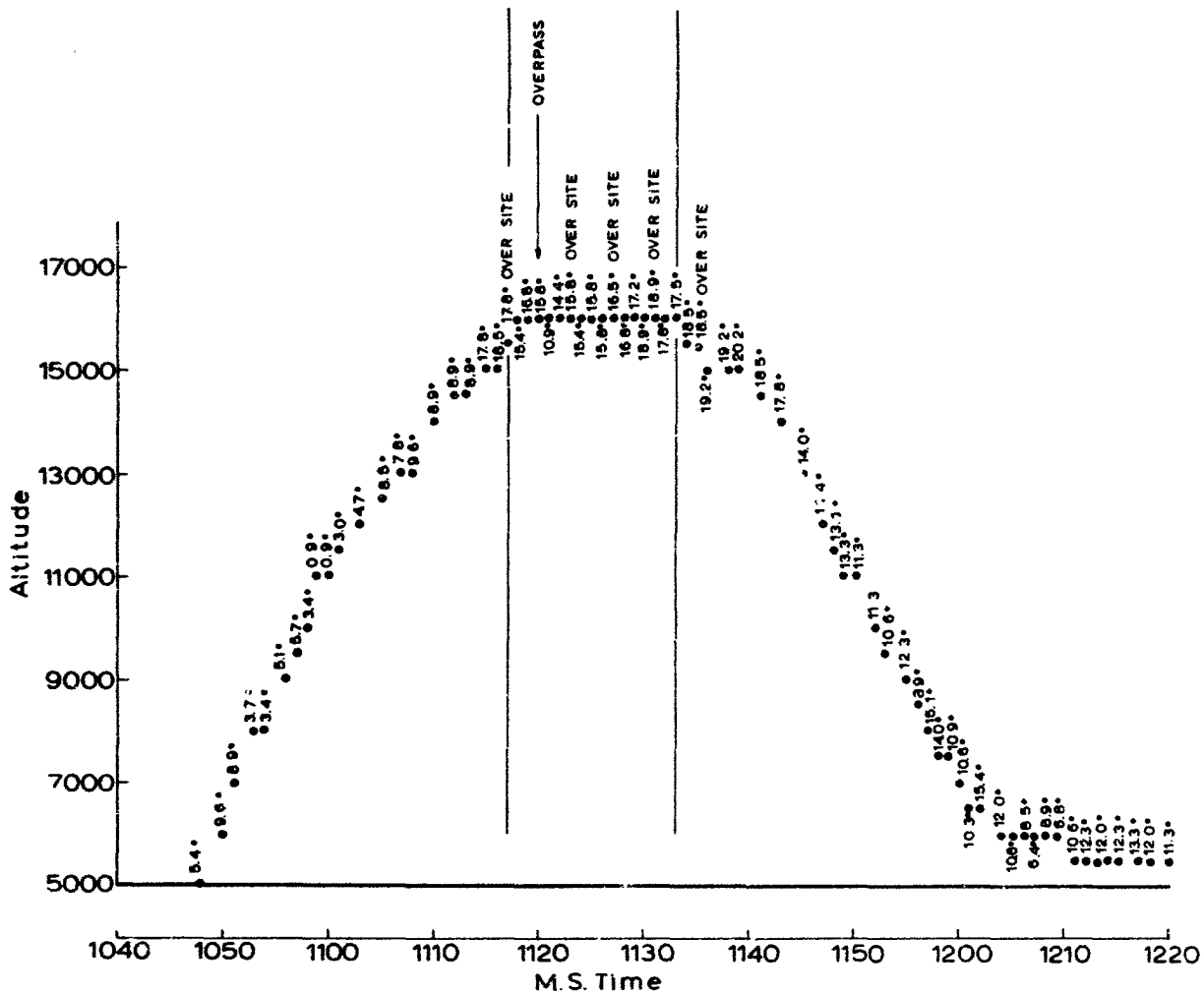

Location	Pawnee Grassland
Orbit	#833
Date	8-14-63
Spectrum	8-13 μ
Temp. Rad	16.2°C
Temp. Soil	26.5°C
Temp. Air	25.6°C
R H	Missing
Cloud Cover	Clear

Fig. 13 Minute averages of black body radiation temperatures measured over grassland from the airborne radiometers.

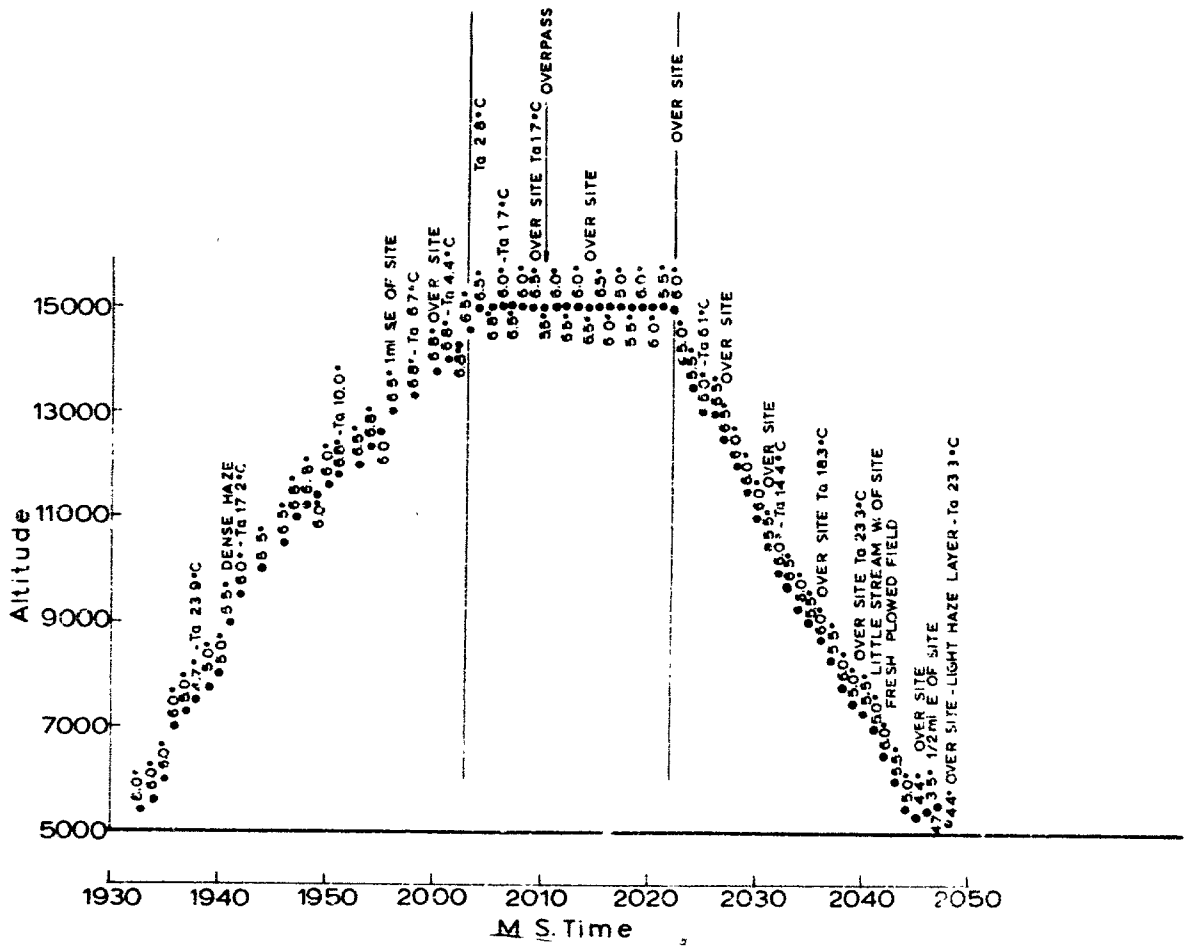

Location	Pawnee Grassland
Orbit	#1548
Date	10-1-63
Spectrum	8-13 μ
Temp. Rad.	6.1°C
Temp. Soil	12.78°C
Temp Air	11.6°C
R.H.	61 %
Cloud Cover	Dense Haze

Fig. 14 Minute averages of blackbody radiation temperatures measured over grassland from the airborne radiometers.

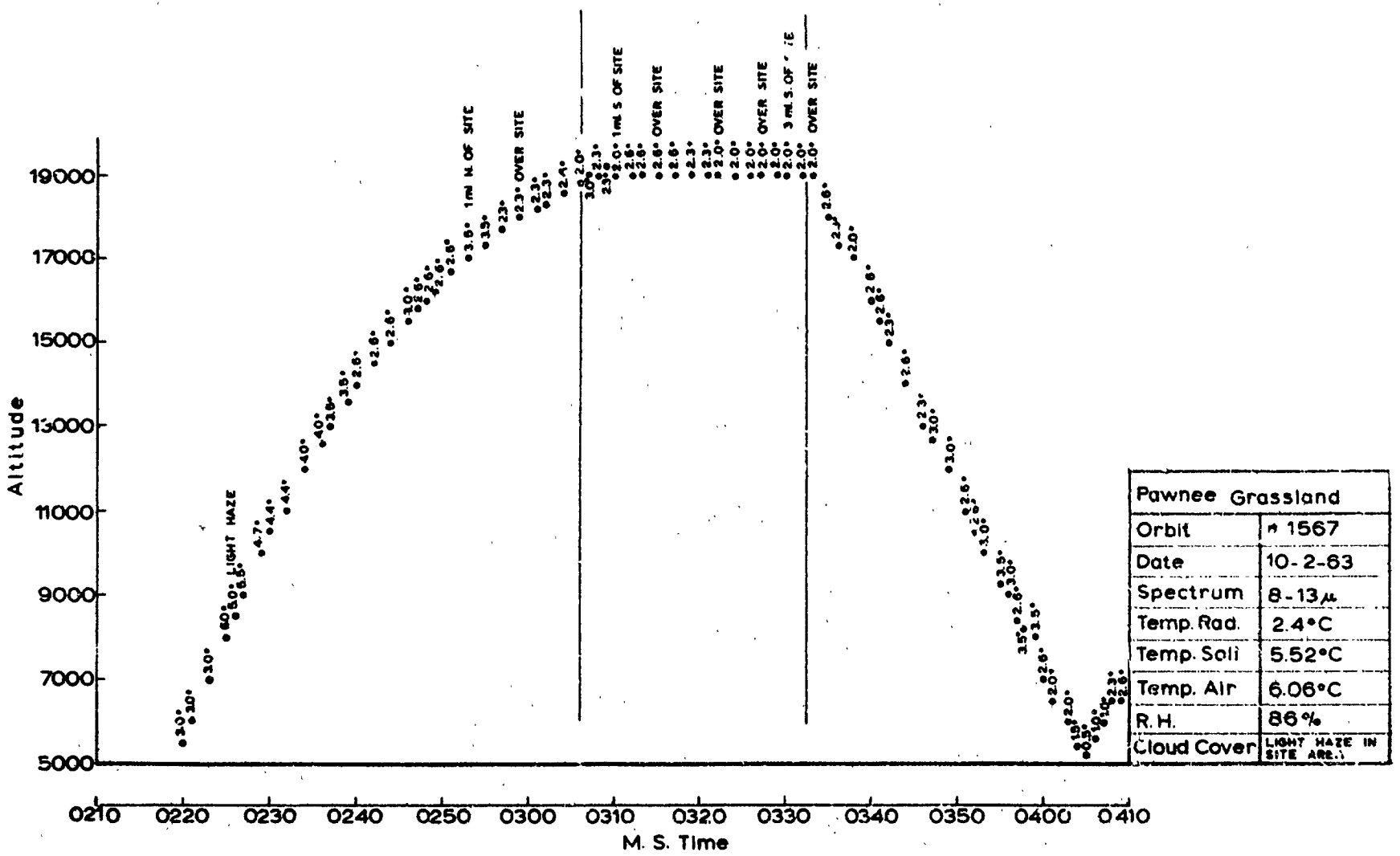

Fig. 15 Minute averages of black body radiation temperatures measured over grassland from the airborne radiometers.

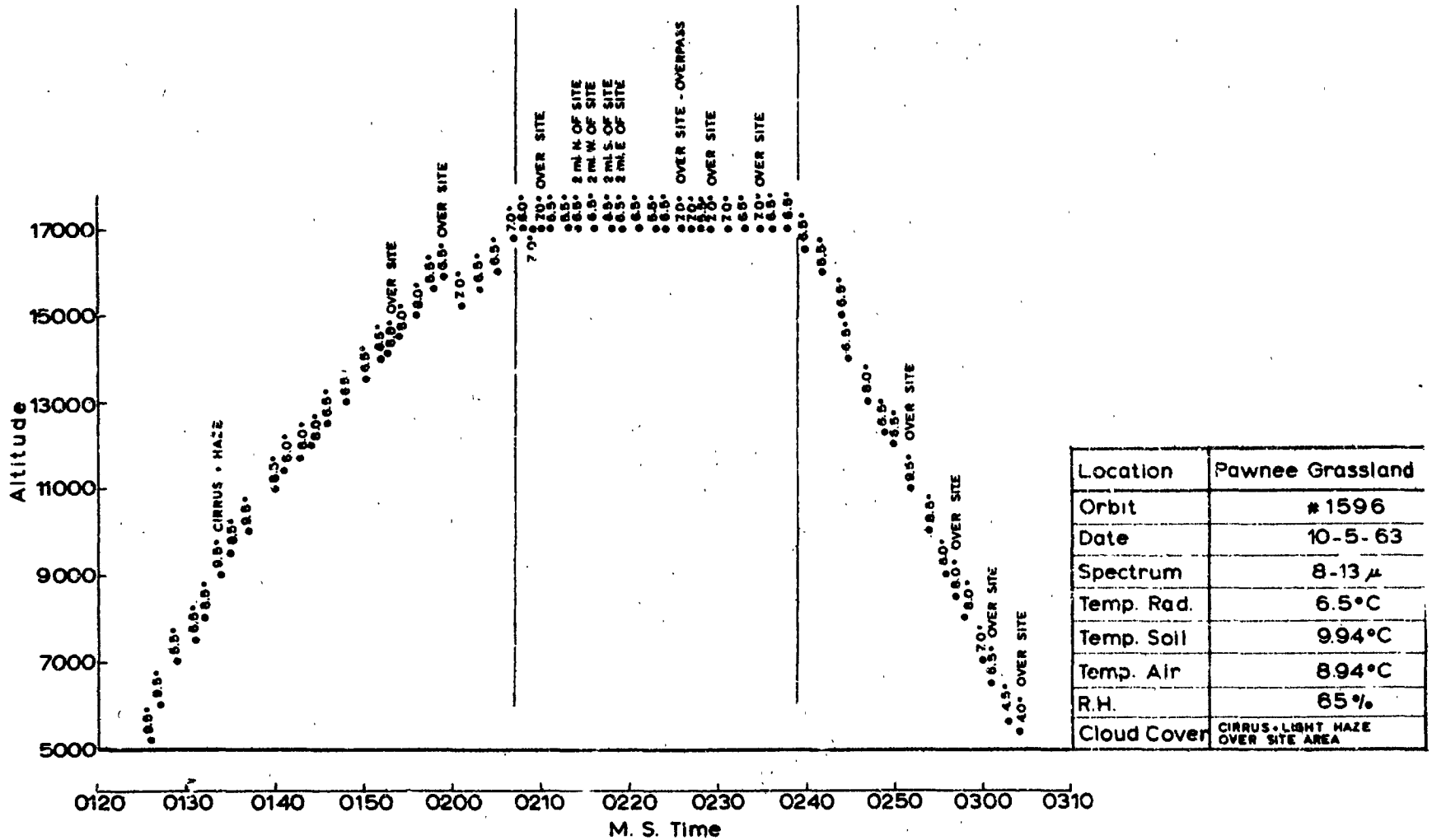

Fig.13. Minute averages of black body radiation temperatures measured over grassland from the airborne radiometers.

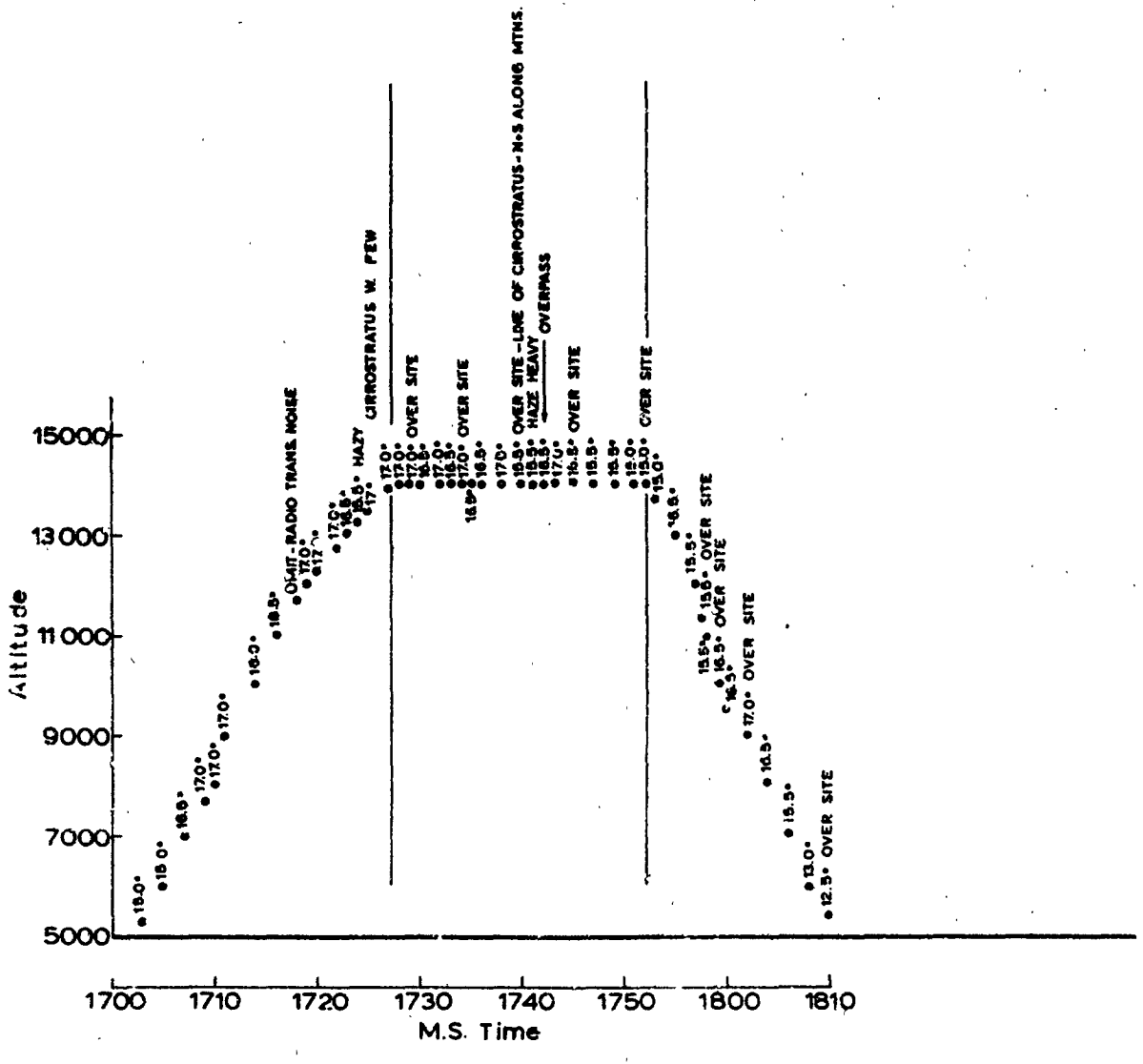

Location	Pawnee Grassland
Orbit	#1650
Date	10-8-63
Spectrum	8-13 μ
Temp. Rad.	16.2°C
Temp. Soil	13.44°C
Temp. Air	16.7° C
R.H.	51 %
Cloud Cover	Haze

Fig. 17 Minute averages of black body radiation temperatures measured over grassland from the airborne radiometers.

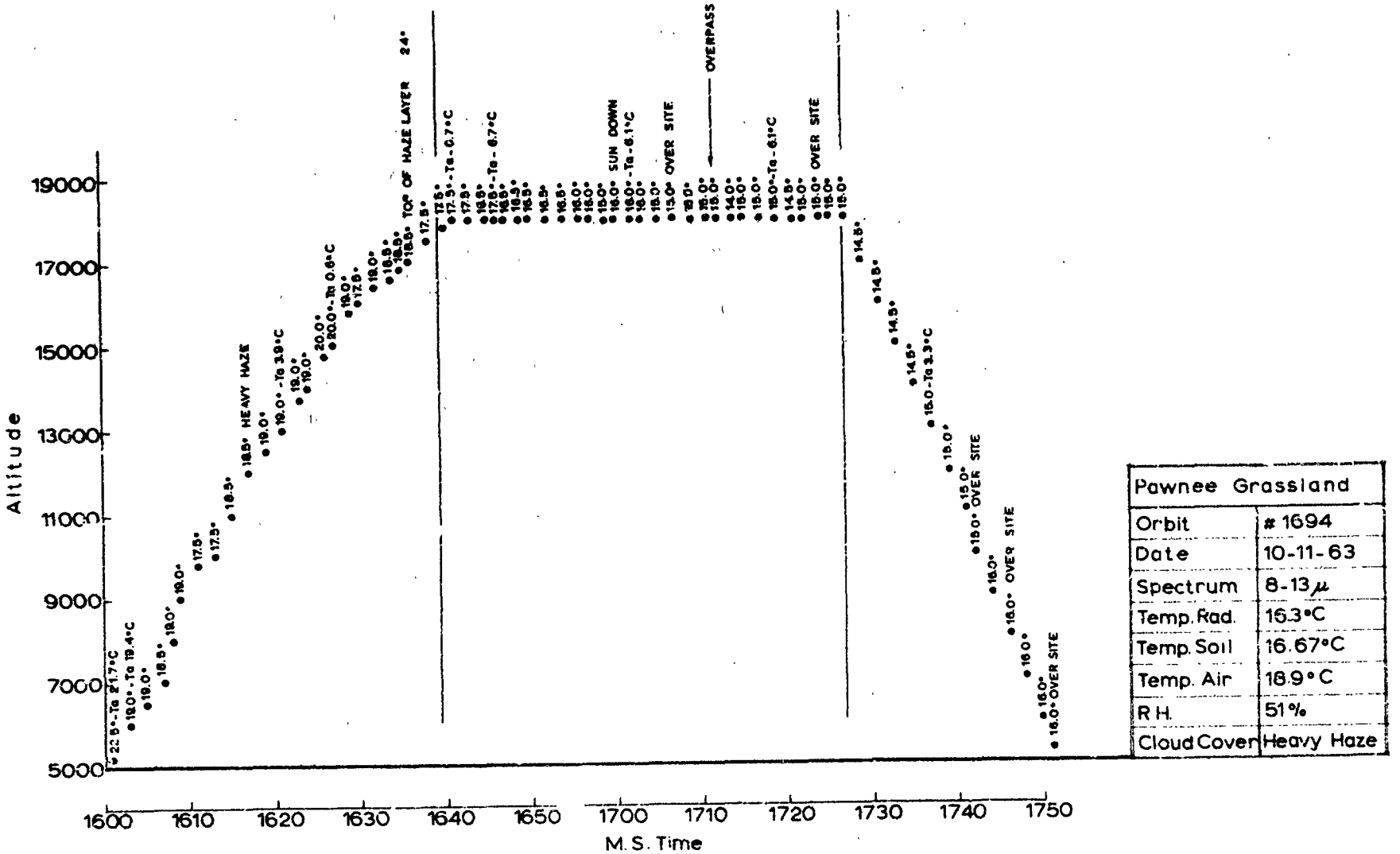

Fig. 13 Minute averages of black body radiation temperatures measured over grassland from the airborne radiometers.

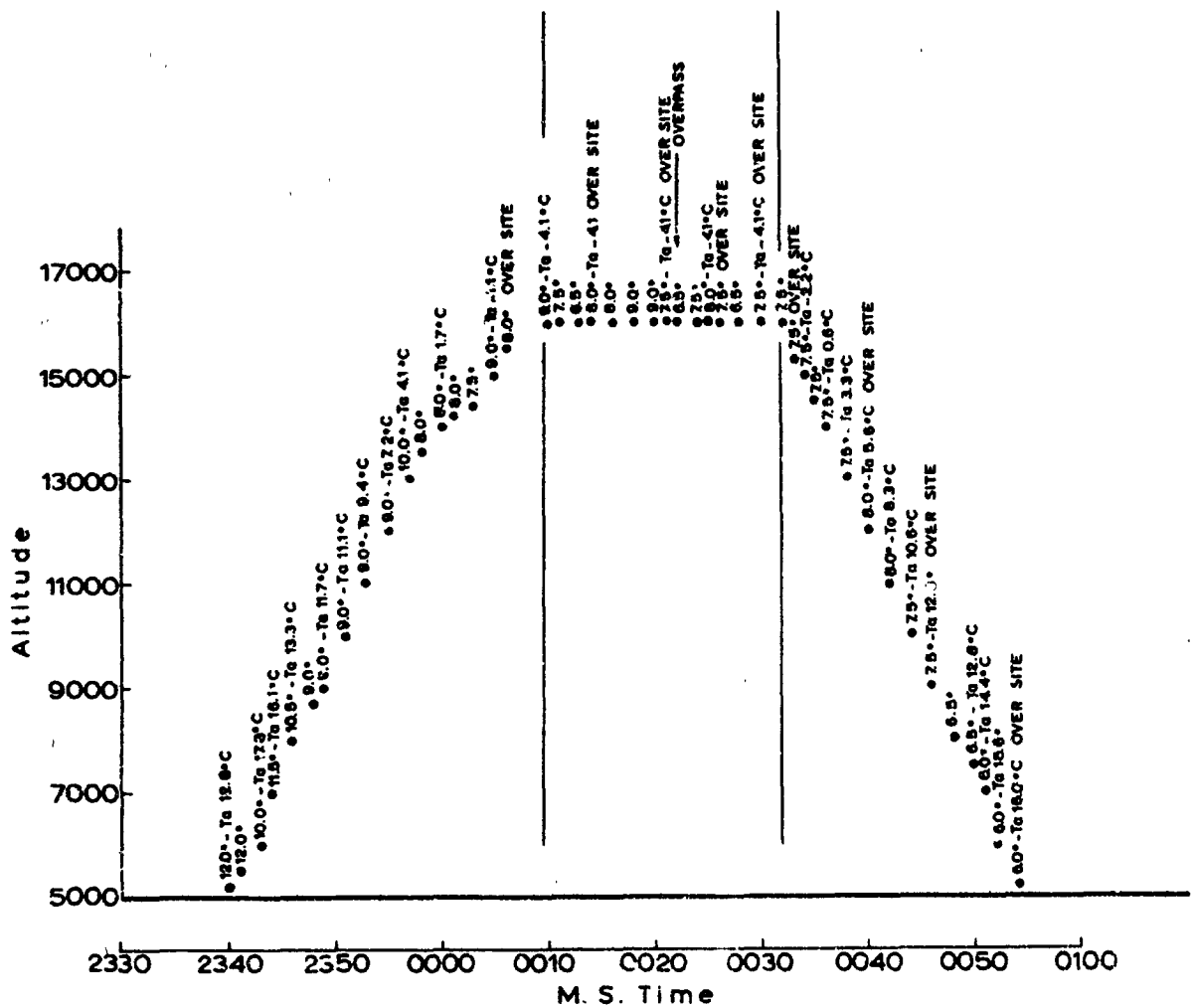

Location	Pawnee Grassland
Orbit	# 1713
Date	10-13-63
Spectrum	8-13 μ
Temp. Rad.	7.7 °C
Temp. Soil	8.6 °C
Temp. Air	8.9 °C
R.H.	59 %
Cloud Cover	Thin Haze

Fig. 19 Minute averages of black body radiation temperatures measured over grassland from the airborne radiometers.

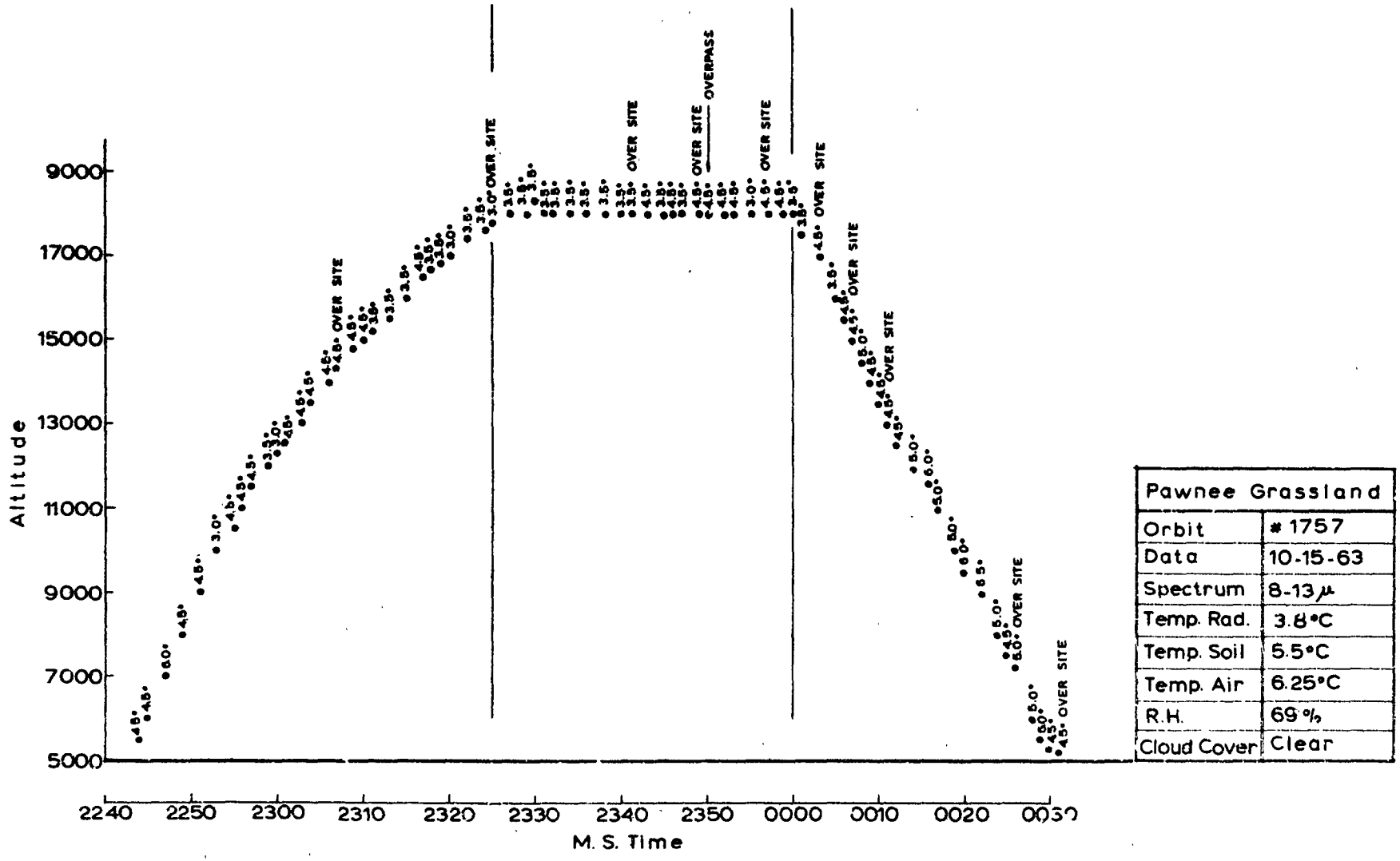

Fig. 20 Minute averages of black body radiation temperatures measured over grassland from the airborne radiometers.

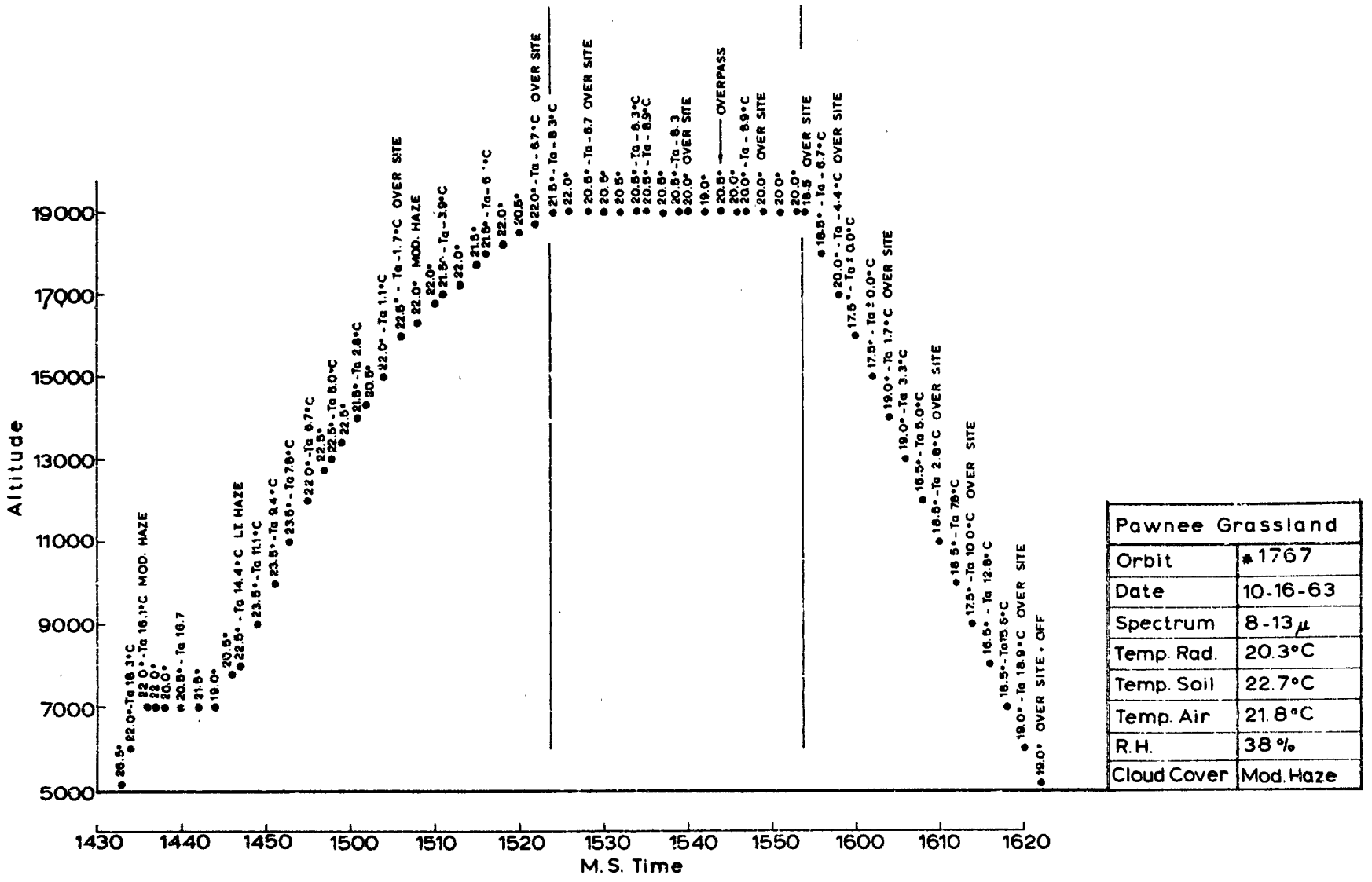

Fig. 21 Minute averages of black body radiation temperatures measured over grassland from the airborne radiometers.

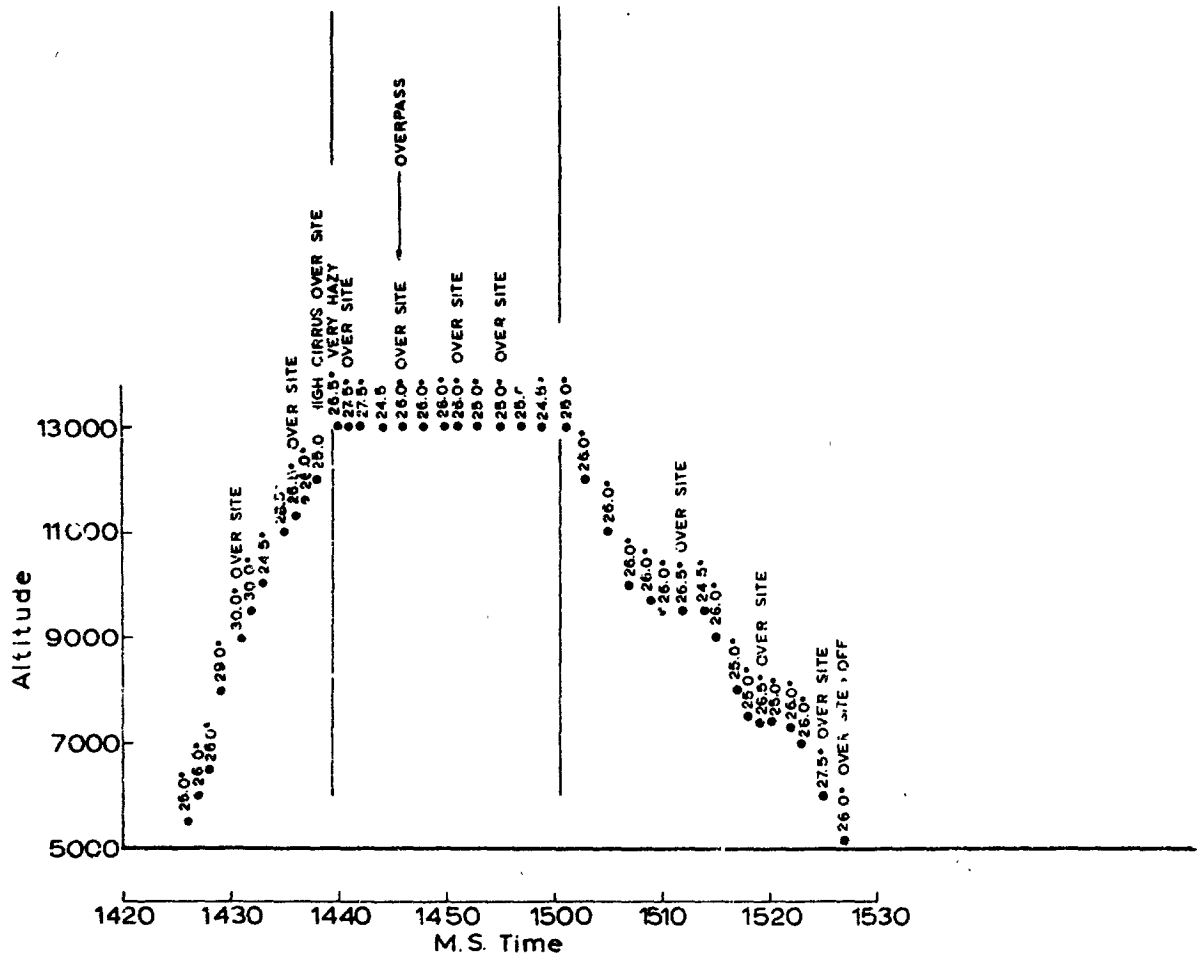

Location	Pawnee Grassland
Orbit	# 1796
Date	10-18-63
Spectrum	8-13 μ
Temp Rad.	25.7°C
Temp. Soil	27.8°C
Temp. Air	25.3°C
R.H.	62 %
Cloud Cover	Mod. Haze

Fig. 22 Minute averages of black body radiation temperatures measured over grassland from the airborne radiometers.

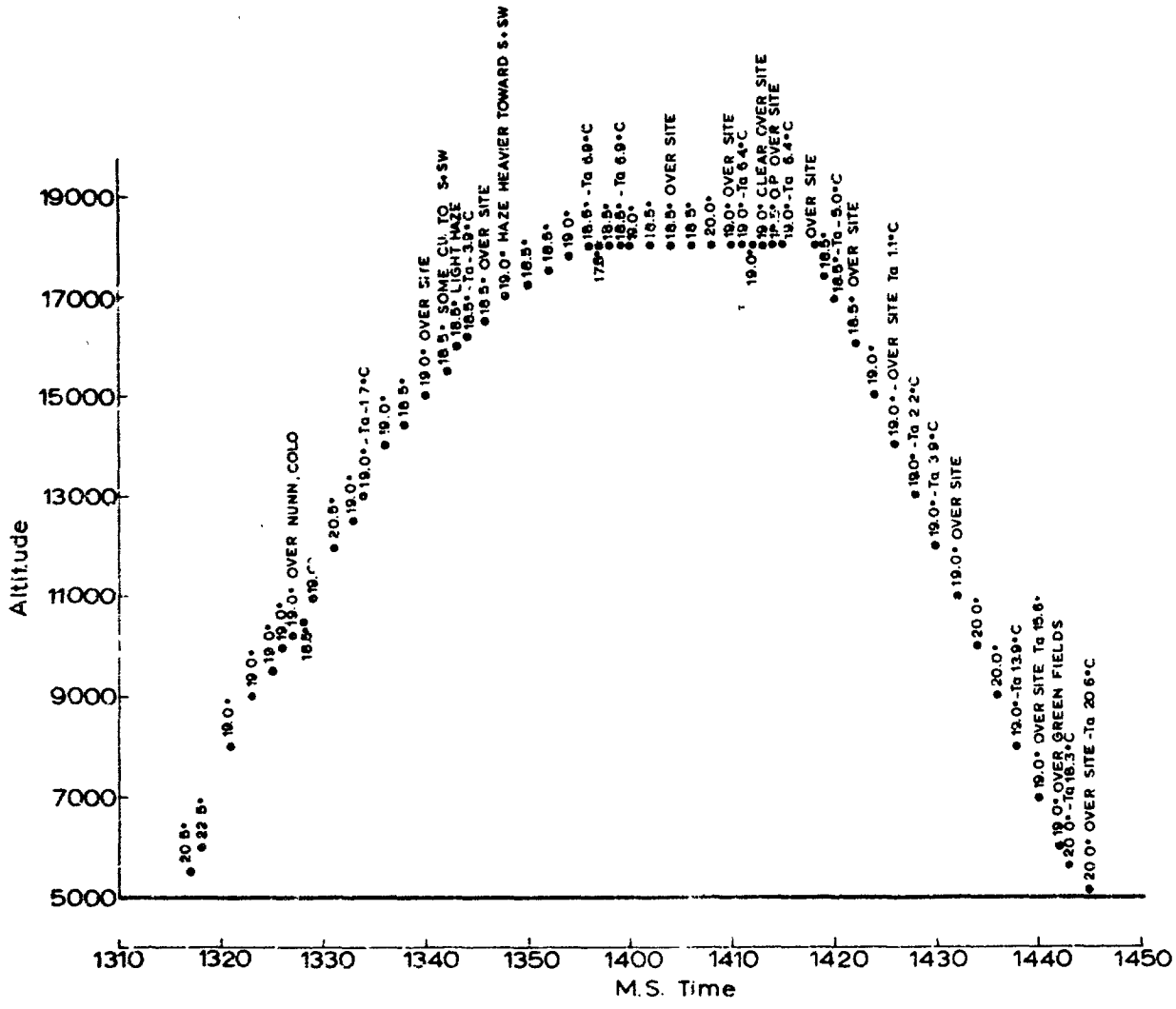

Location	Pawnee Grassland
Orbit	1840
Date	10-21-63
Spectrum	8-13 μ
Temp Rad	18.7° C
Temp. Soil	31.1° C
Temp. Air	26.7°C
R H.	32.5 %
Cloud Cover	Light Haze

Fig. 23 Minute averages of black body radiation temperatures measured over grassland from the airborne radiometers.

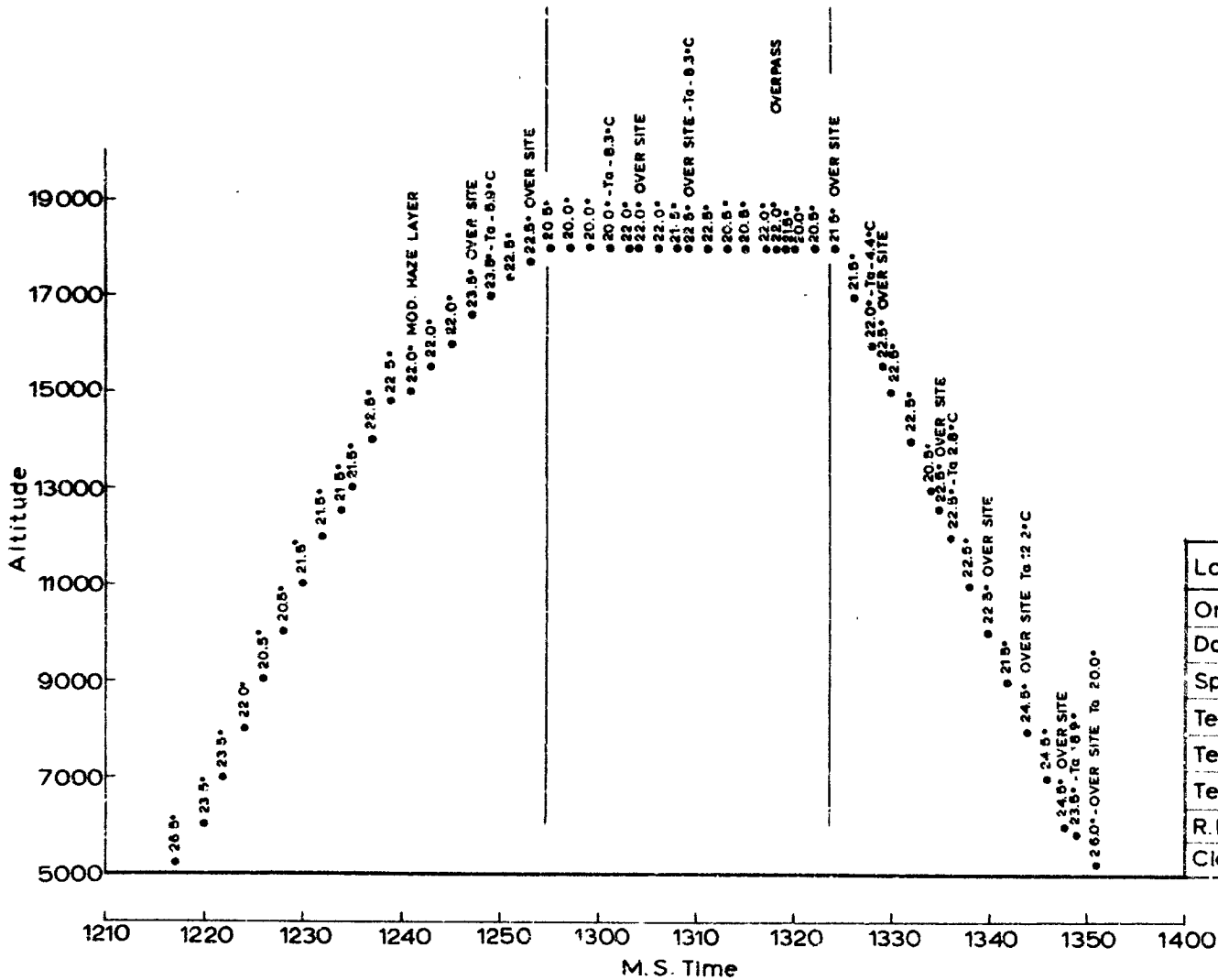

Location	Pawnee Grassland
Orbit	# 1869
Date	10-23-63
Spectrum	8-13 μ
Temp. Rad.	21.2°C
Temp. Soil	33.5°C
Temp Air	22.4°C
R.H	35%
Cloud Cover	Mod. Haze

Fig. 24 Minute averages of black body radiation temperatures measured over grassland from the airborne radiometers.

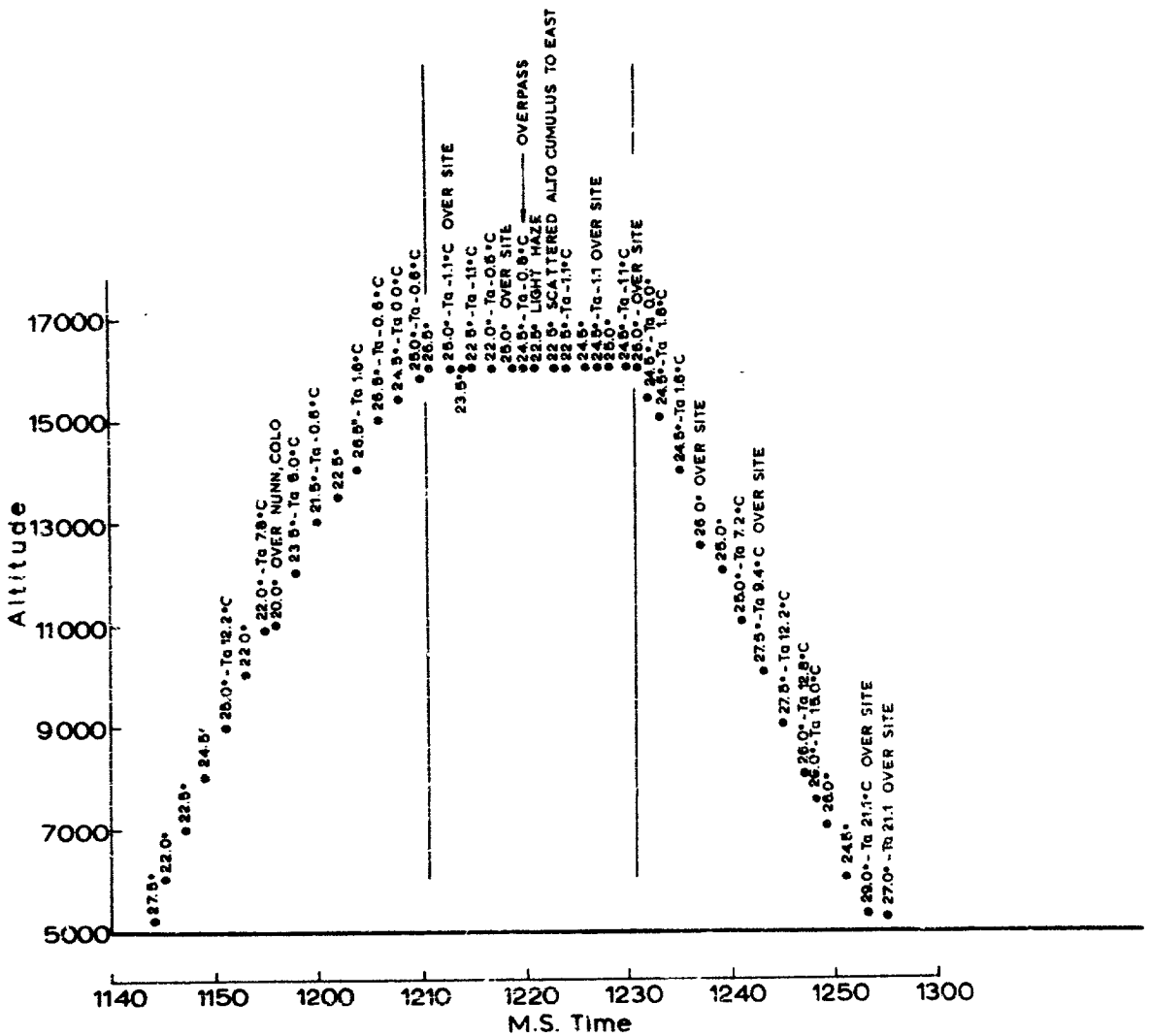

Location	Pawnee Grassland
Orbit	# 1898
Date	10-25-63
Spectrum	8-13 μ
Temp. Rad.	24.0°C
Temp. Soil	26.5°C
Temp. Air	22.33°C
R.H	39.5%
Cloud Cover	Light Haze

Fig. 25 Minute averages of black body radiation temperatures measured over grassland from the airborne radiometers.

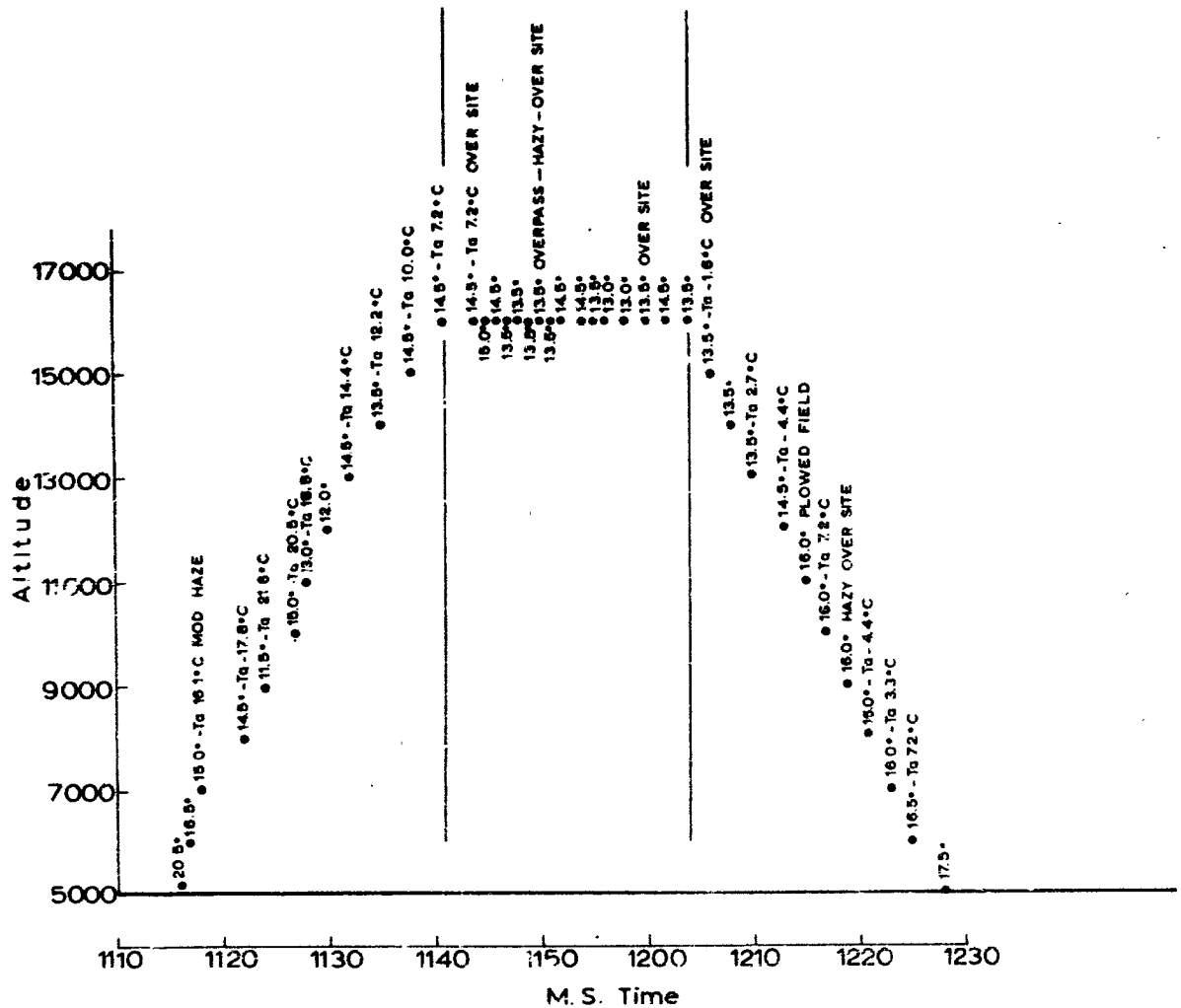

Location	Pawnee Grassland
Orbit	# 1942
Date	10-28-63
Spectrum	8-13μ
Temp. Rad	13.9°C
Temp. Soil	18.5°C
Temp. Air	9.1°C
R H	52 %
Clou Cover	Mod Haze

Fig. 23 Minute averages of black body radiation temperatures measured over grassland from the airborne radiometers.

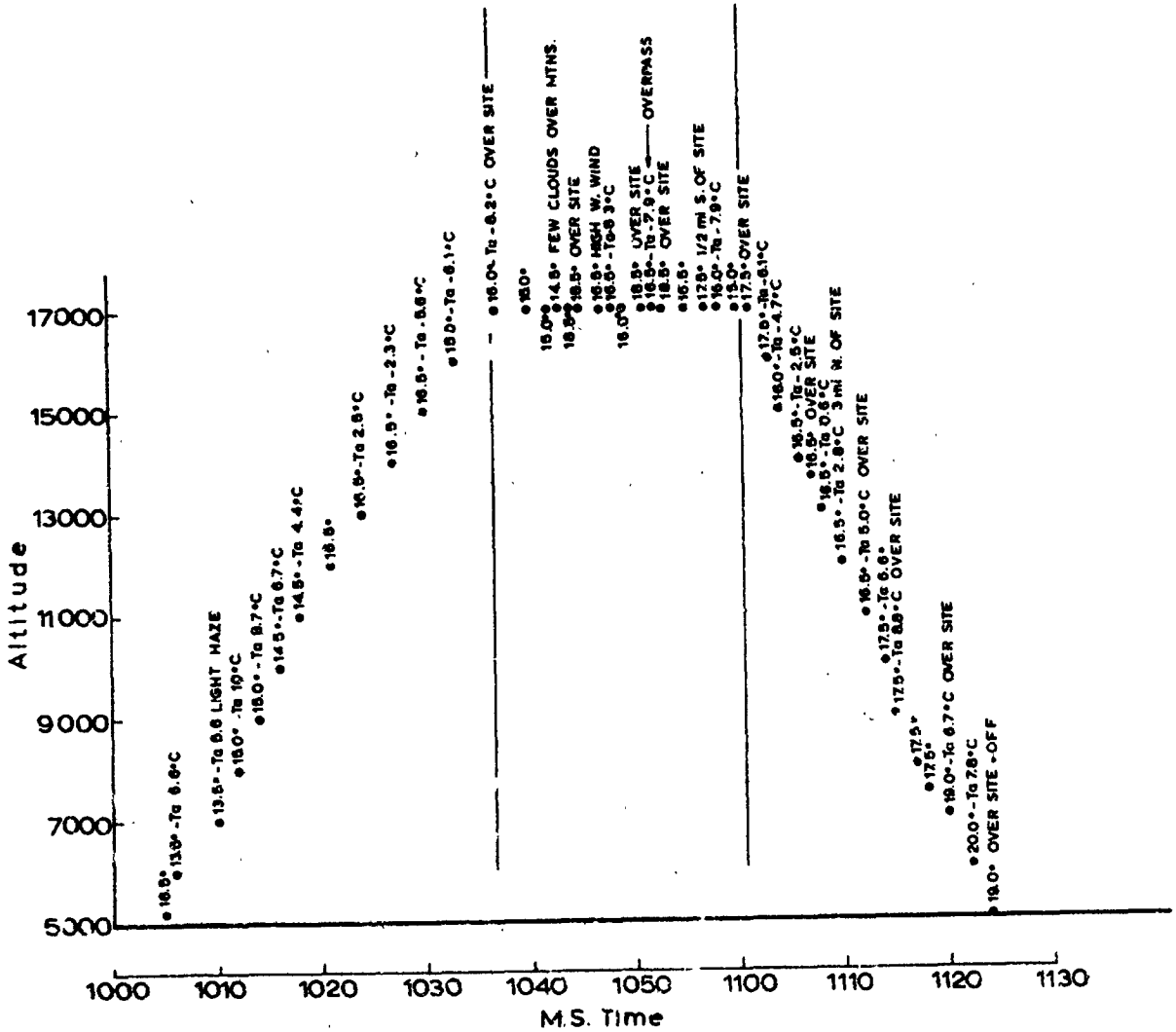

Location	Pawnee Grassland
Orbit	# 1971
Date	10-30-63
Spectrum	8-13 μ
Temp. Rad.	16.7°C
Temp. Soil	24.8°C
Temp Air	12.4°C
R.H.	66 %
Cloud Cover	LIGHT HAZE IN GENERAL SITE AREA
Wind	4-5 Kts

Fig. 27 Minute averages of black body radiation temperatures measured over grassland from the airborne radiometers.

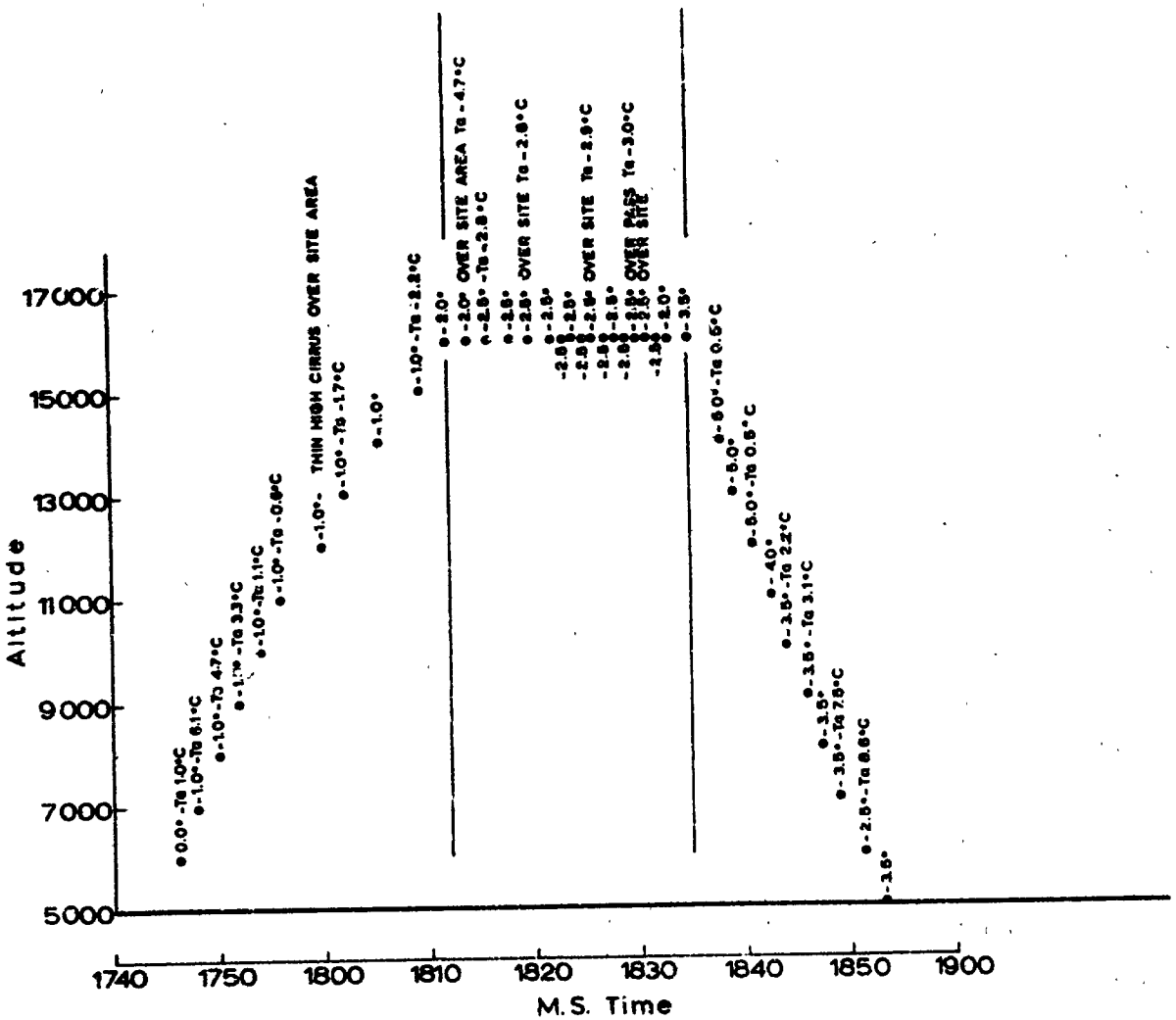

Location	Pawnee Grassland
Orbit	# 2005
Date	11-1-63
Spectrum	8-13μ
Temp. Rad.	-2.47°C
Temp. Soil	-0.39°C
Temp. Air	-6.7°C
R.H.	98.5%
Cloud Cover	THIN HIGH SCATTERED CIRRUS OVER SITE AREA

Fig. 23 Minute averages of black body radiation temperatures measured over grassland from the airborne radiometers.

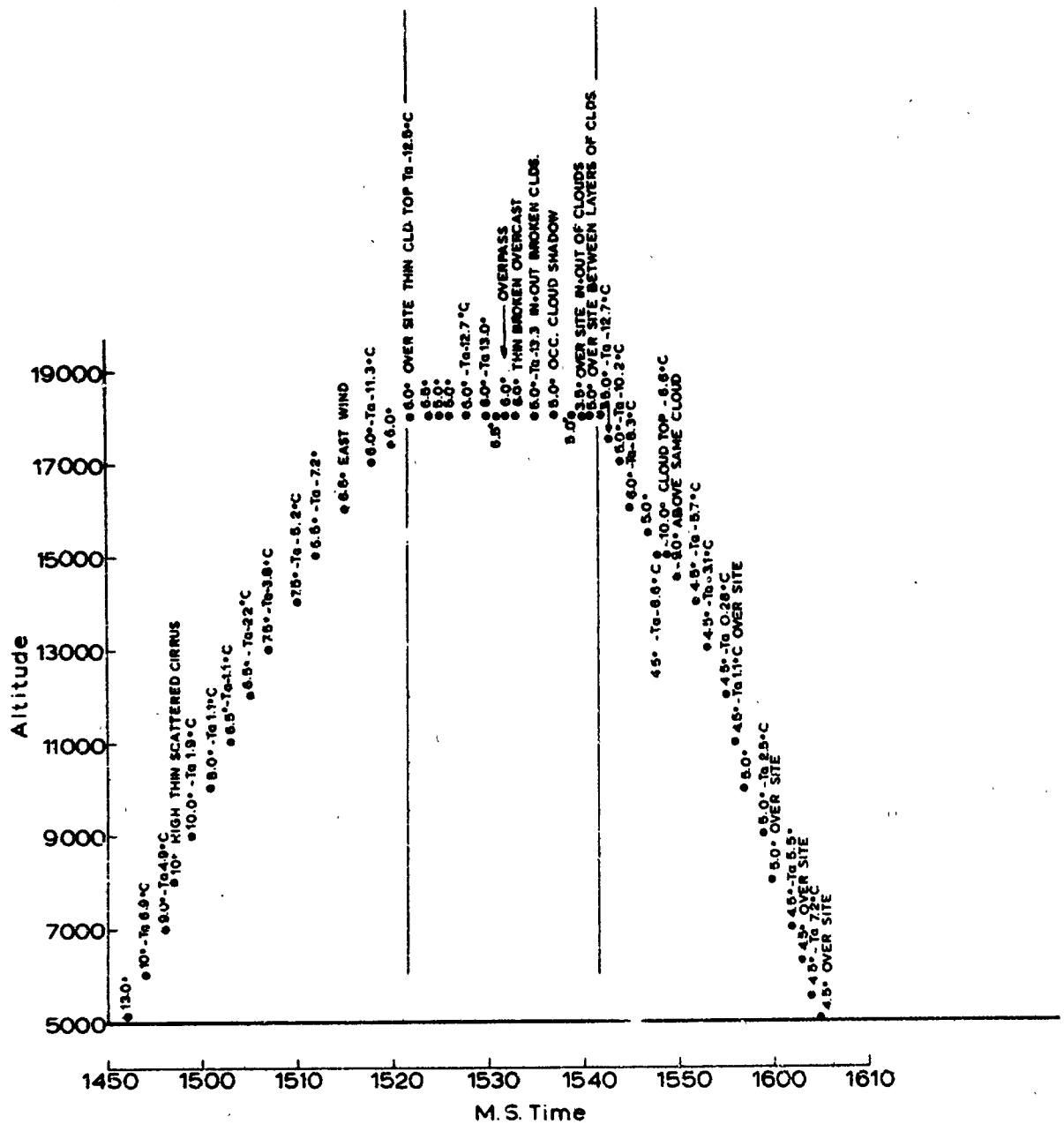

Location	Pawnee Grassland
Orbit	# 2151
Date	11-11-63
Spectrum	8-13 μ
Temp. Rad.	5.4° C
Temp. Soil	7.7° C
Temp. Air	8.6° C
R.H.	96 %
Cloud Cover	ALTOSTRATUS OVER SITE AREA
Wind	70 mph(est.)

Fig. 29 Minute averages of black body radiation temperatures measured over grassland from the airborne radiometers.

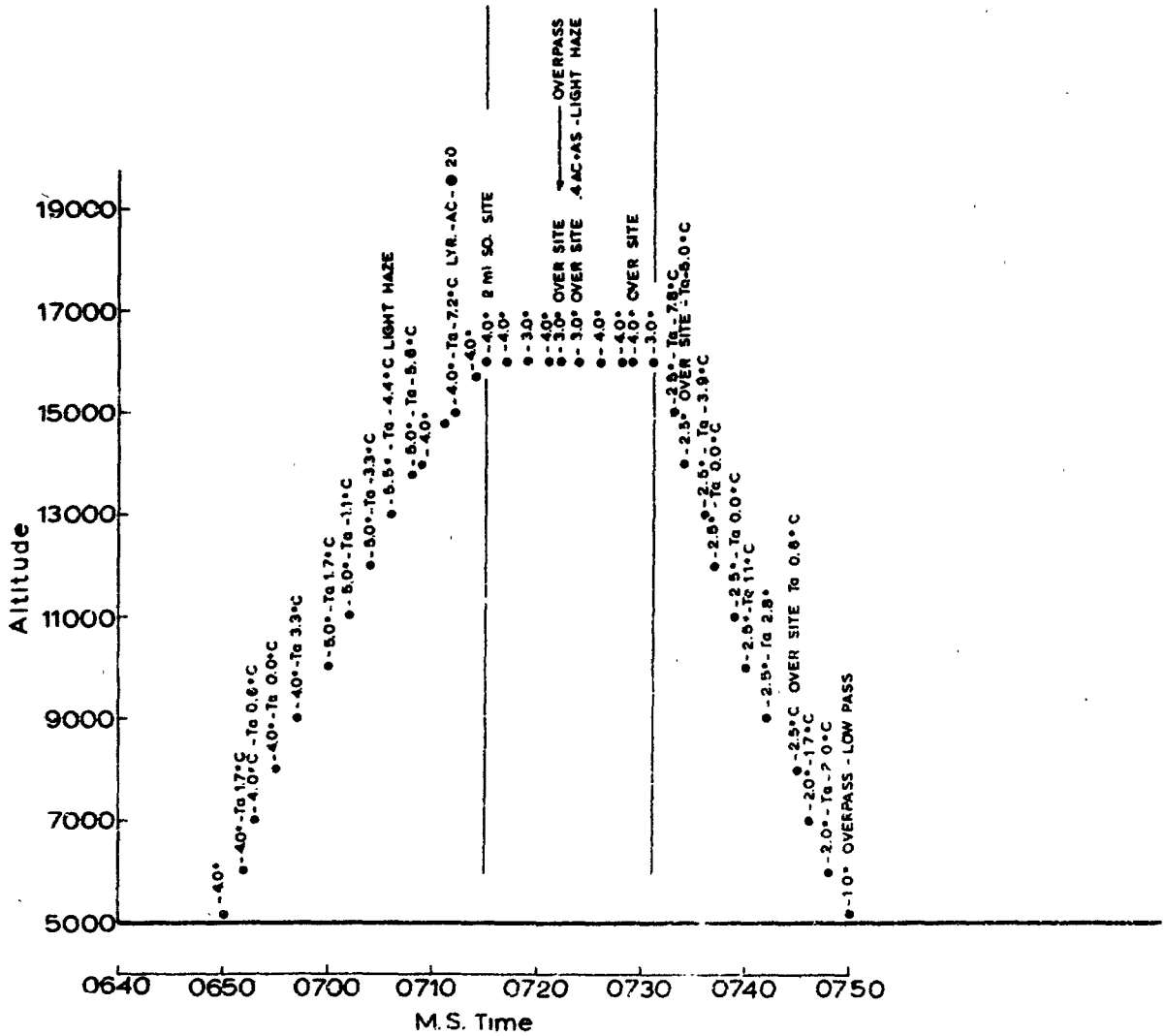

Location	Pawnee Grassland
Orbit	# 2161
Date	11-12-63
Spectrum	8-13 μ
Temp. Rad.	-3.6°C
Temp. Soil	-2.4°C
Temp. Air	-3.0°C
R.H.	78 %
Cloud Cover	.4AC+AS Light Haze
Wind	5-10 mph

Fig. 30 Minute averages of black body radiation temperatures measured over grassland from the airborne radiometers.

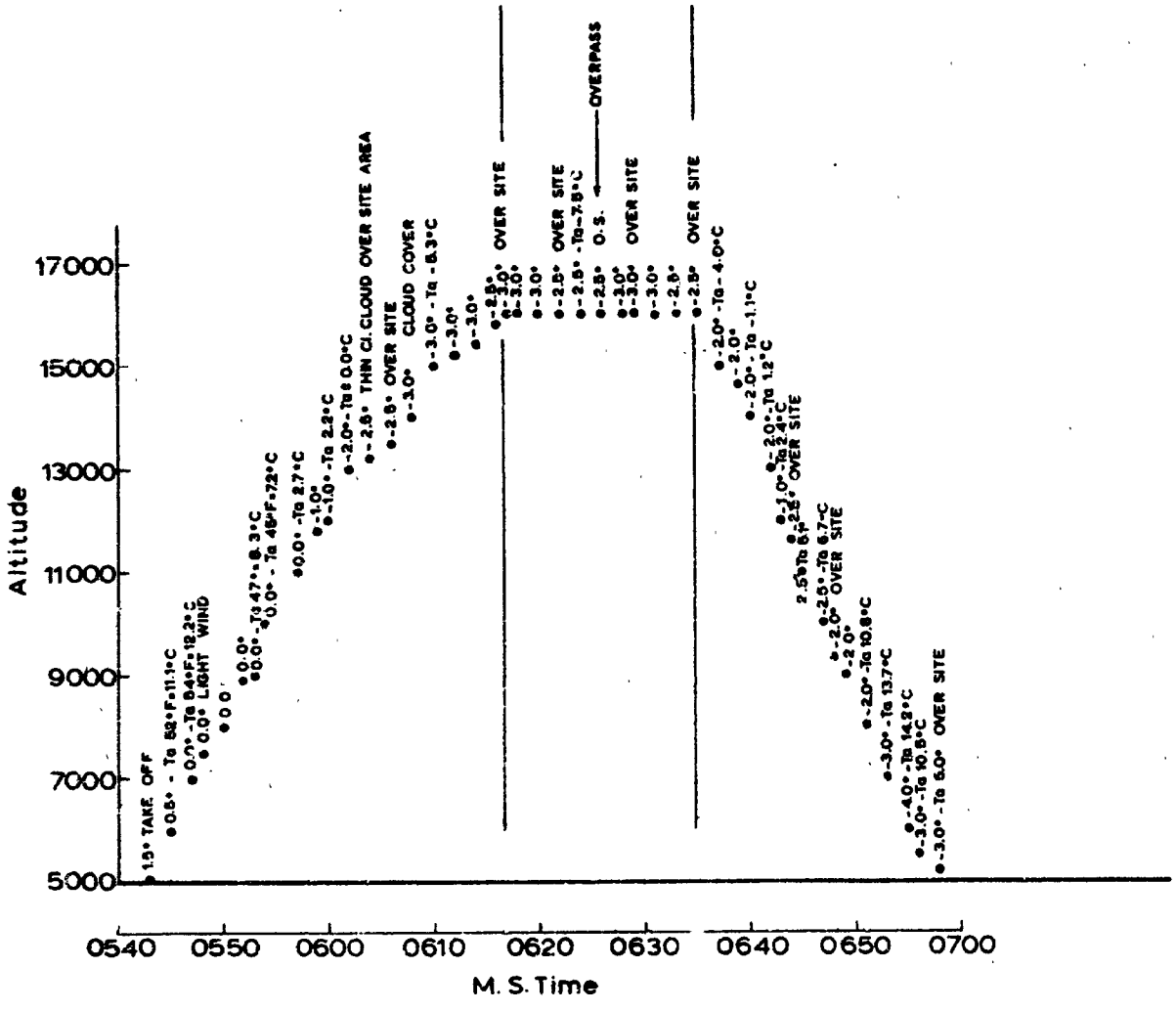

Location	Pawnee Grassland
Orbit	# 2190
Date	11-14-63
Spectrum	8-13 μ
Temp. Rad.	-2.7°C
Temp. Soil	-2.8°C
Temp. Air	-3.7°C
R.H	89 %
Cloud Cover	Thin Cirrus

Fig. 31 Minute averages of black body radiation temperatures measured over grassland from the airborne radiometers.

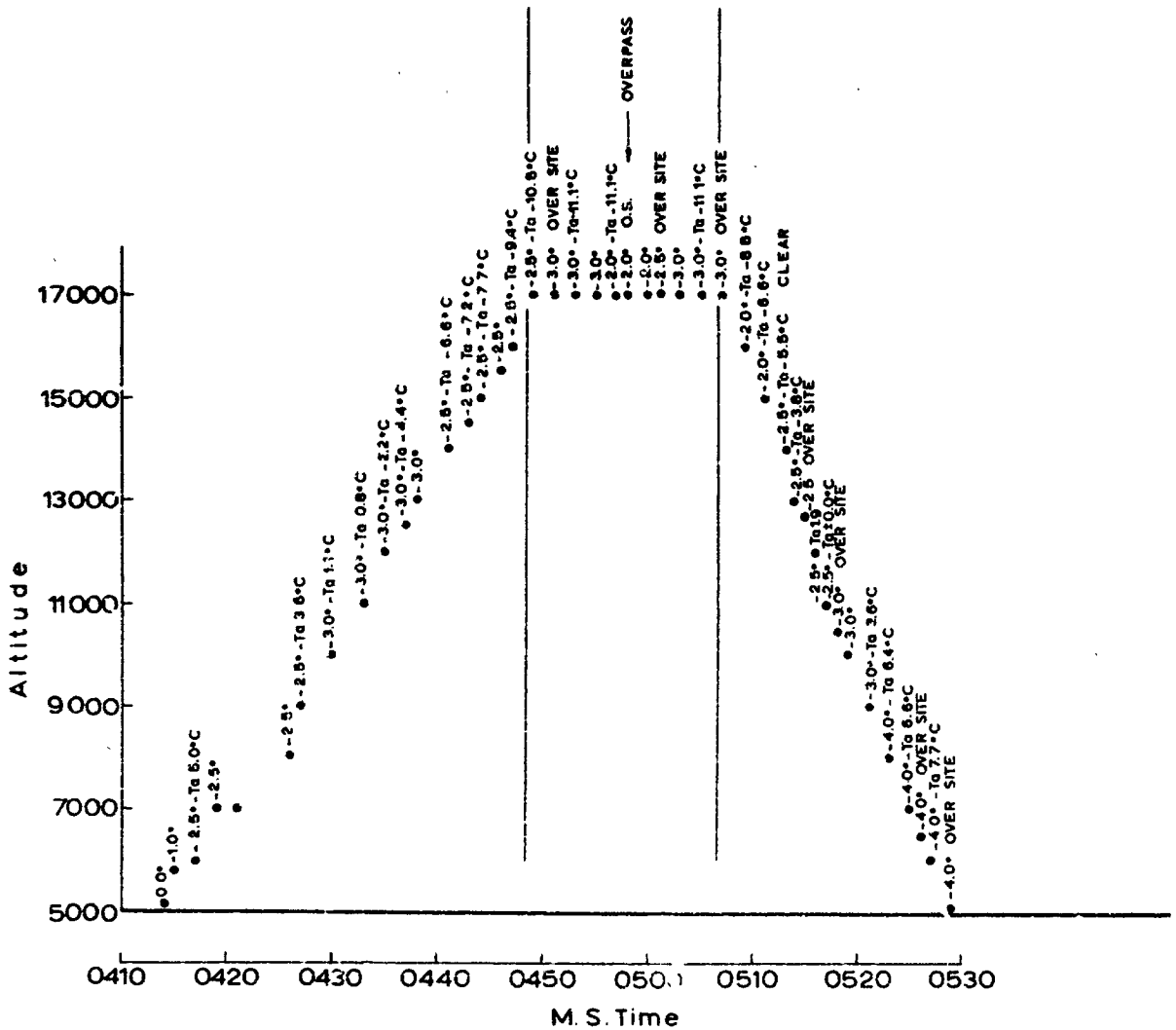

Location	Pawnee Grassland
Orbit	2263
Date	11-19-63
Spectrum	8-13μ
Temp. Rad.	-2.6°
Temp. Soil	- 7.12 °C
Temp. Air	- 9.0 °C
R.H.	82 %
Cloud Cover	CLEAR

Fig. 32 Minute averages of black body radiation temperatures measured over grassland from the airborne radiometers.

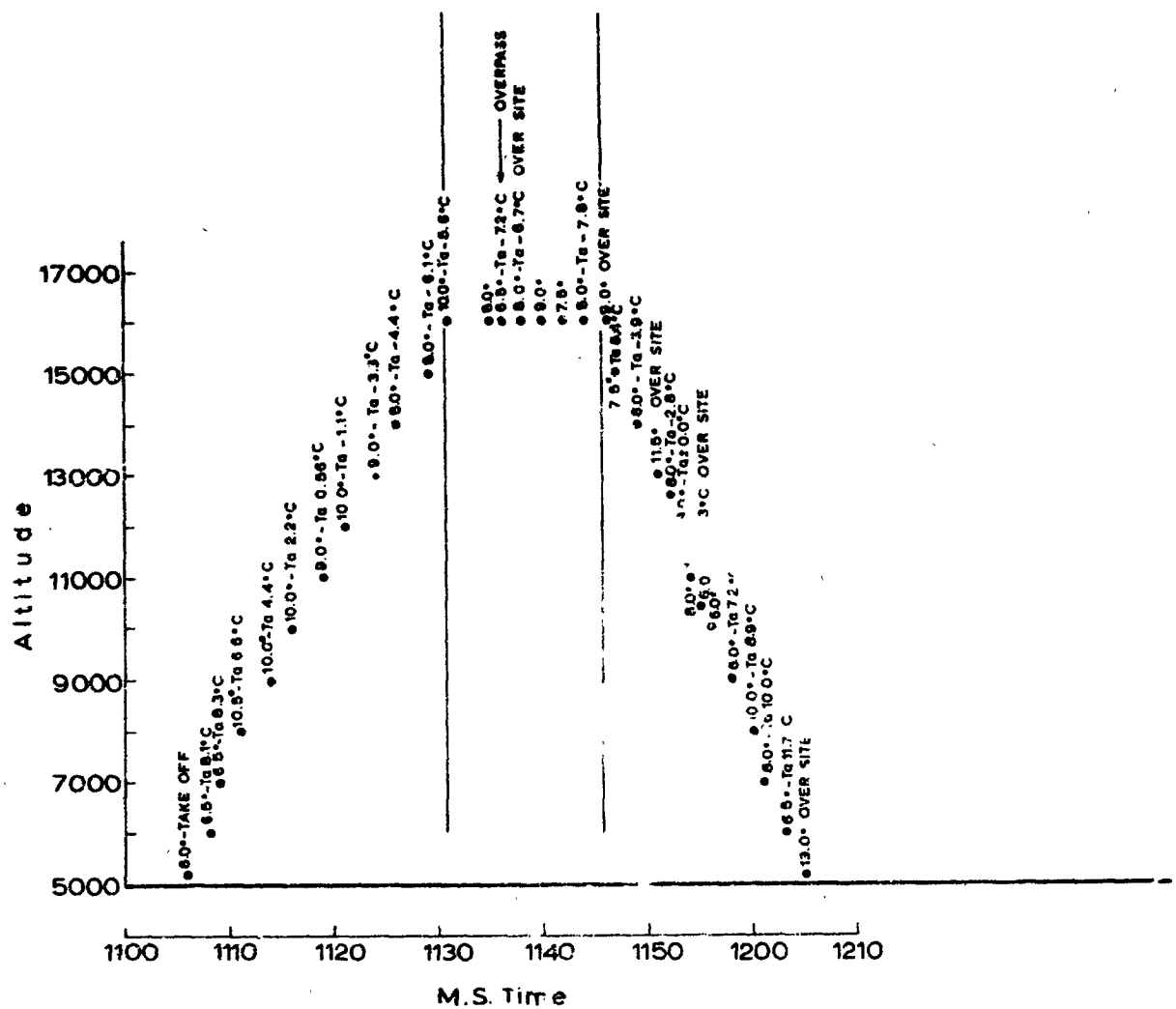

Location	Pawnee Grassland
Orbit	# 2326
Date	11-23-63
Spectrum	8-13μ
Temp. Rad	8.3°C
Temp. Soil	10.3°C
Temp. Air	14.4°C
R.H.	78 %
Cloud Cover	CLEAR

Fig. 33 Minute averages of black body radiation temperatures measured over grassland from the airborne radiometers.

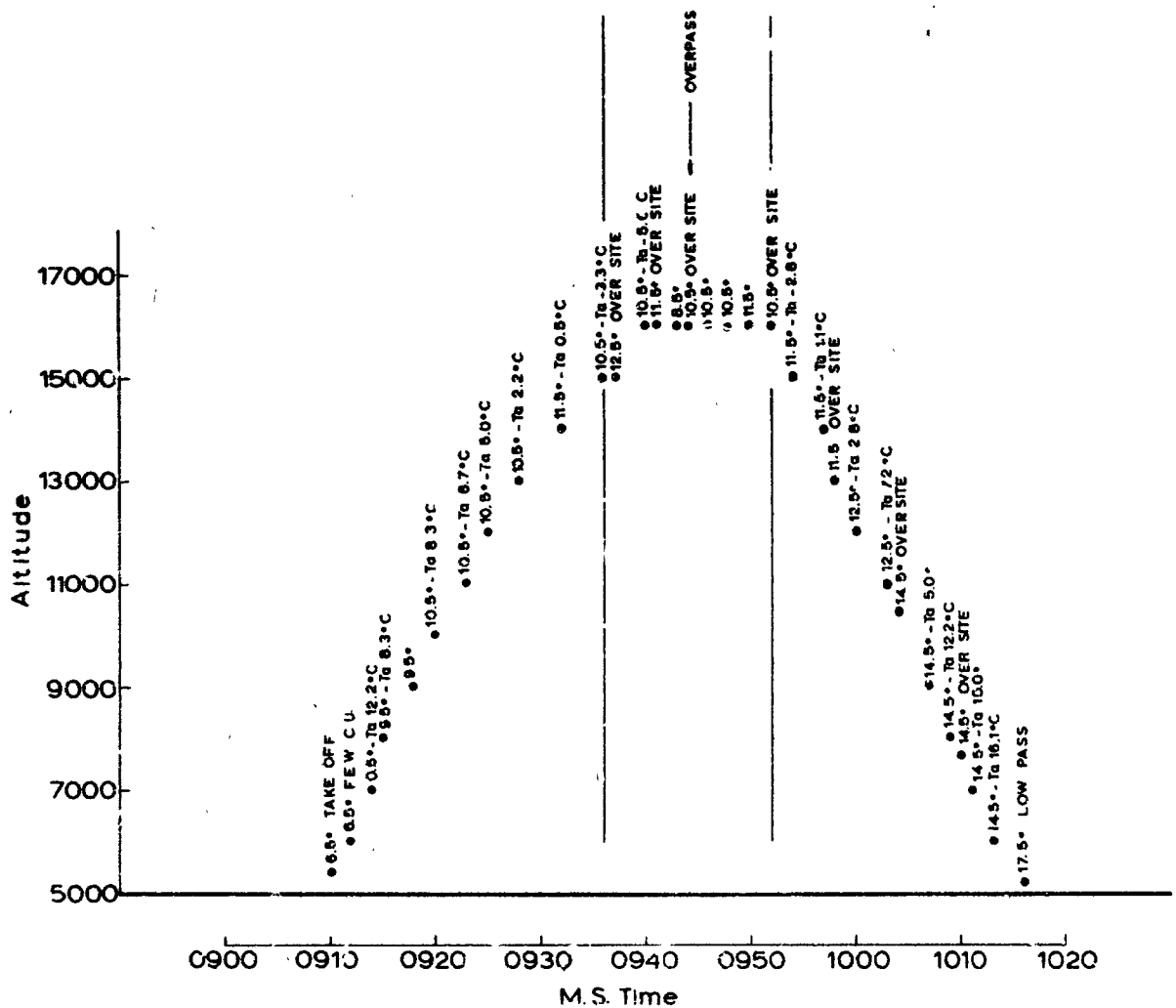

Location	Pawnee Grassland
Orbit	# 2384
Date	11-27-63
Spectrum	8-13 μ
Temp. Rad	10.5°C
Temp. Soil	12.0°C
Temp. Air	12.9°C
R.H.	87 %
Cloud Cover	FEW C.U SCATTERED IN SITE AREA

Fig. 34 Minute averages of black body radiation temperatures measured over grassland from the airborne radiometers.

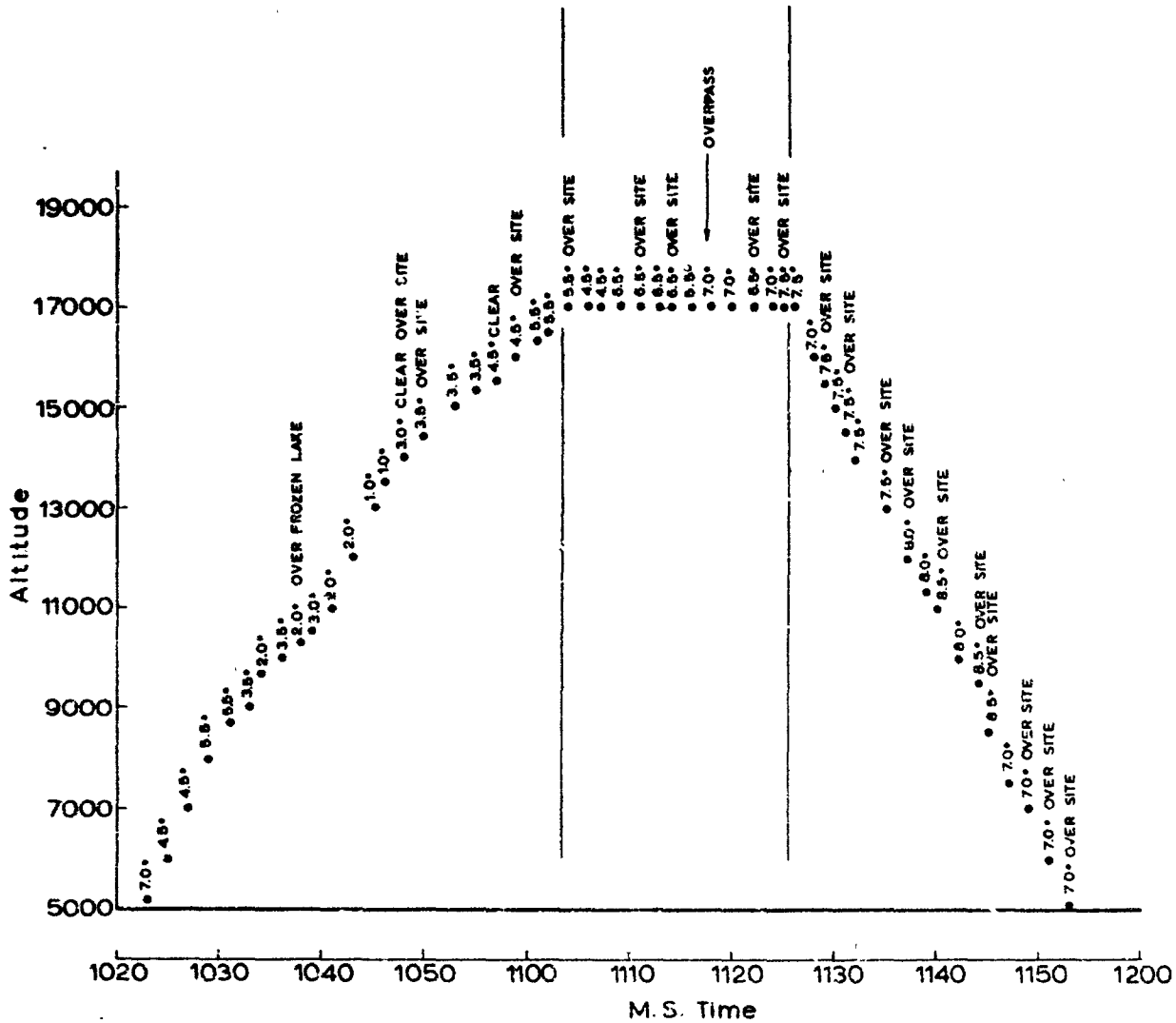

Location	Pawnee Grassland
Orbit	# 3080
Date	1-13-64
Spectrum	8-13 μ
Temp. Rad	6.3°C
Temp. Soil	8.3°C
Temp. Air	0.6°C
R.H.	Missing
Cloud Cover	Clear

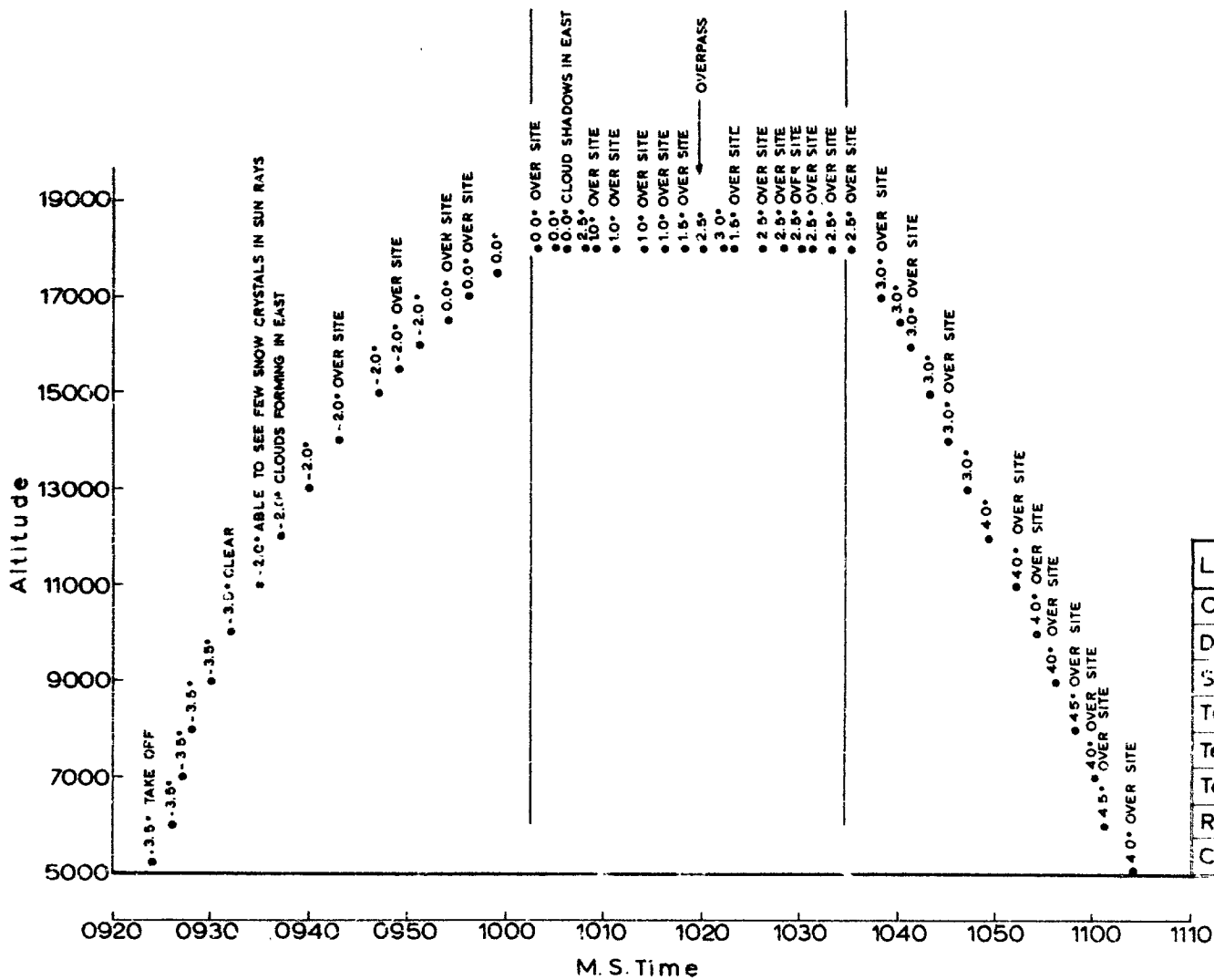

Location	Pawnee Grassland
Orbit	# 3109
Date	1-15-64
Spectrum	8-13 μ
Temp. Rad	1.7°C
Temp. Soil	4.4°C
Temp. Air	-0.6°C
R.H.	Missing
Cloud Cover	Clear

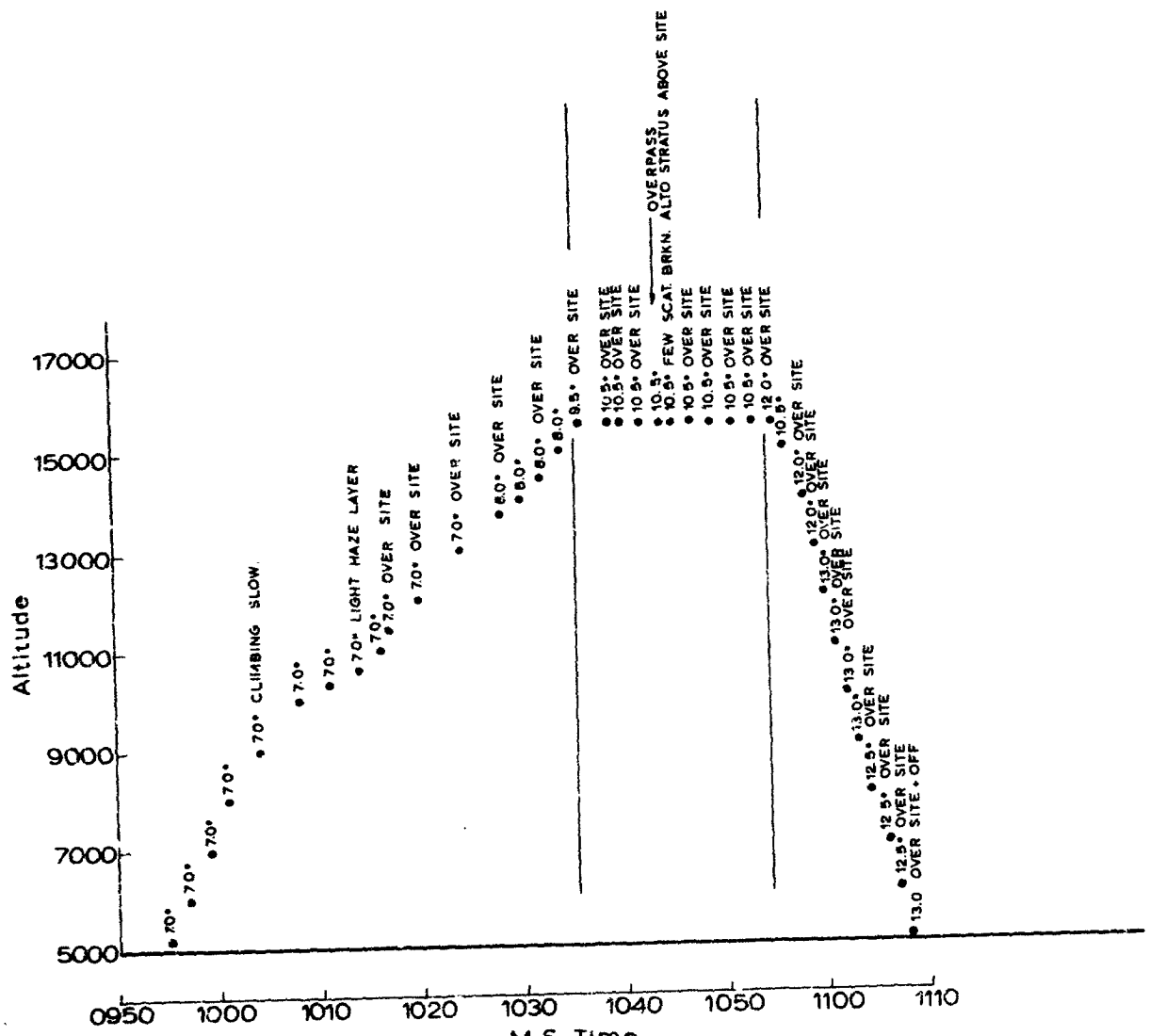

Location	Pawnee Grassland
Orbit	# 3124
Date	1-16-64
Spectrum	8-13 μ
Temp. Rad.	10.5°C
Temp. Soil	8.9°C
Temp. Air	5.3°C
R.H	53%
Cloud Cover	LIGHT HAZE LAYER OVER SITE AREA

Fig. 37 Minute averages of black body radiation temperatures measured over grassland from the airborne radiometers.

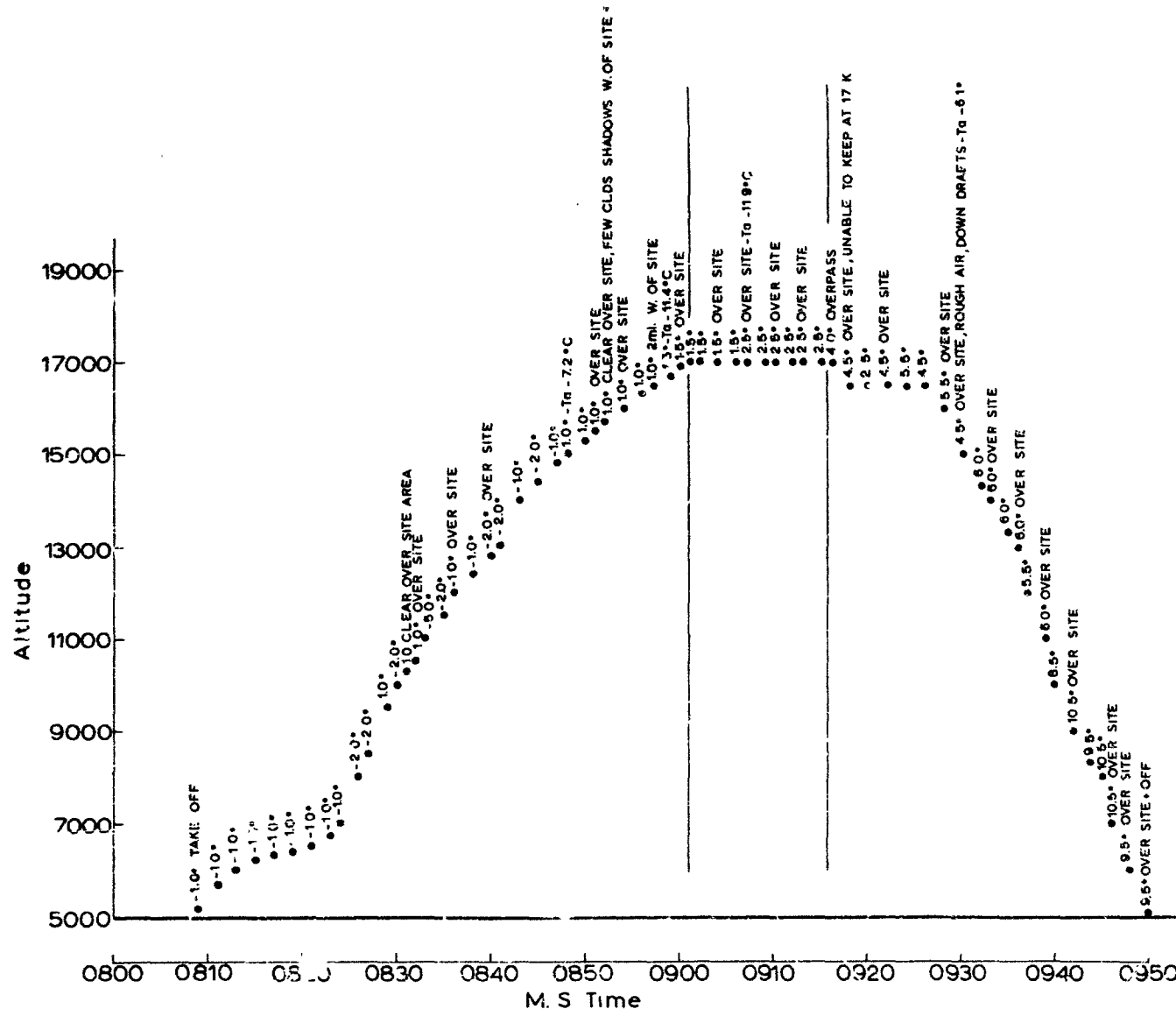

Pawnee Grassland	
Orbit	# 3197
Date	1-21-64
Spectrum	8-13 μ
Temp Rad.	2.3°C
Temp. Soil	3.0°C
Temp. Air	14.2°C
R.H	27.5°C
Cloud Cover	FEW HIGH CLDS.

Fig. 38 Minute averages of black body radiation temperatures measured over grassland from the airborne radiometers.

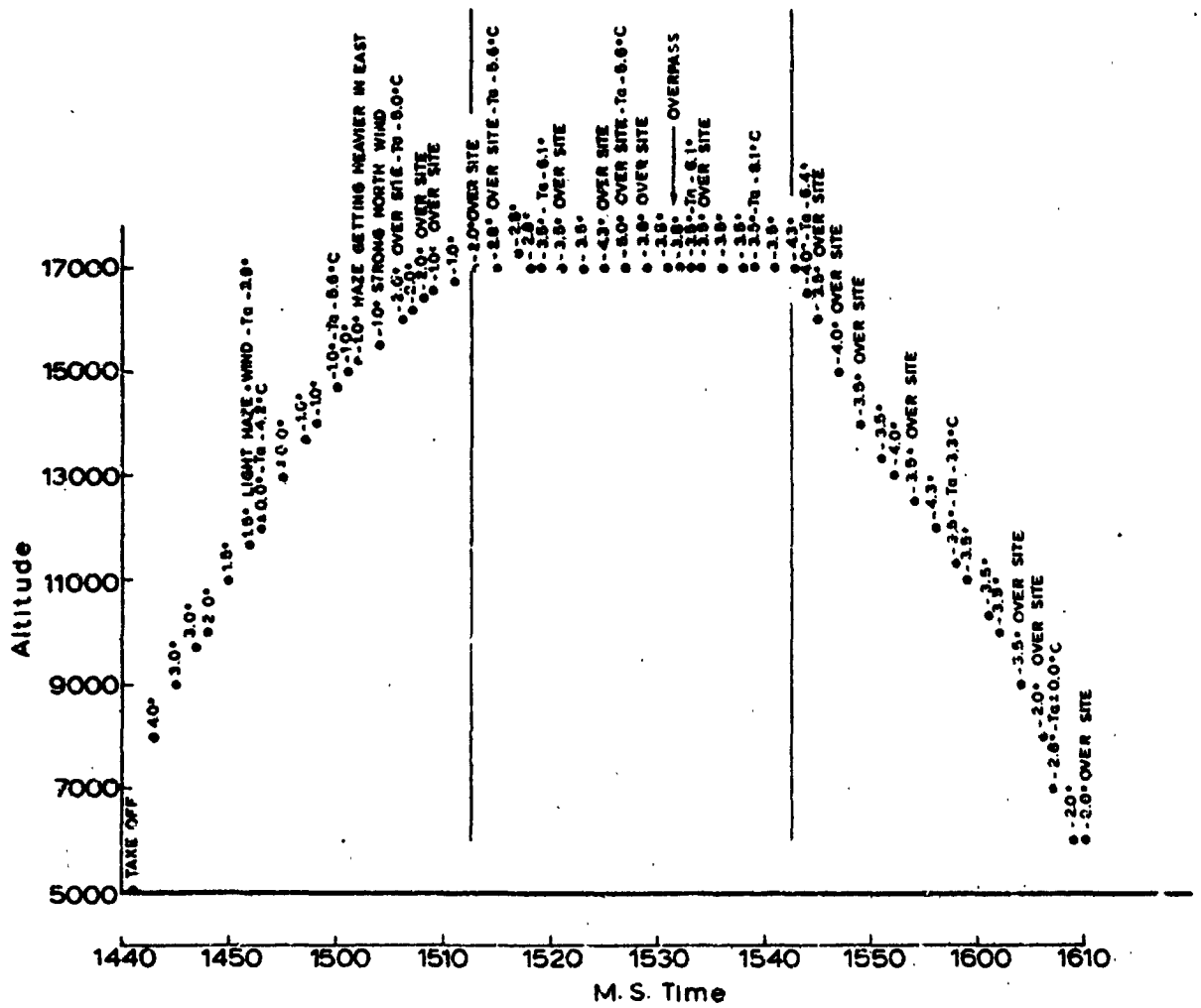

Location	Pawnee Grassland
Orbit	# 3245
Date	1-24-64
Spectrum	8-13 μ
Temp. Rad.	- 3.5°C
Temp. Soil	- 3.1°C
Temp. Air	- 2.8°C
R.H.	38 %
Cloud Cover	1/10 SC AND 1/10 AC OVER MTNS.

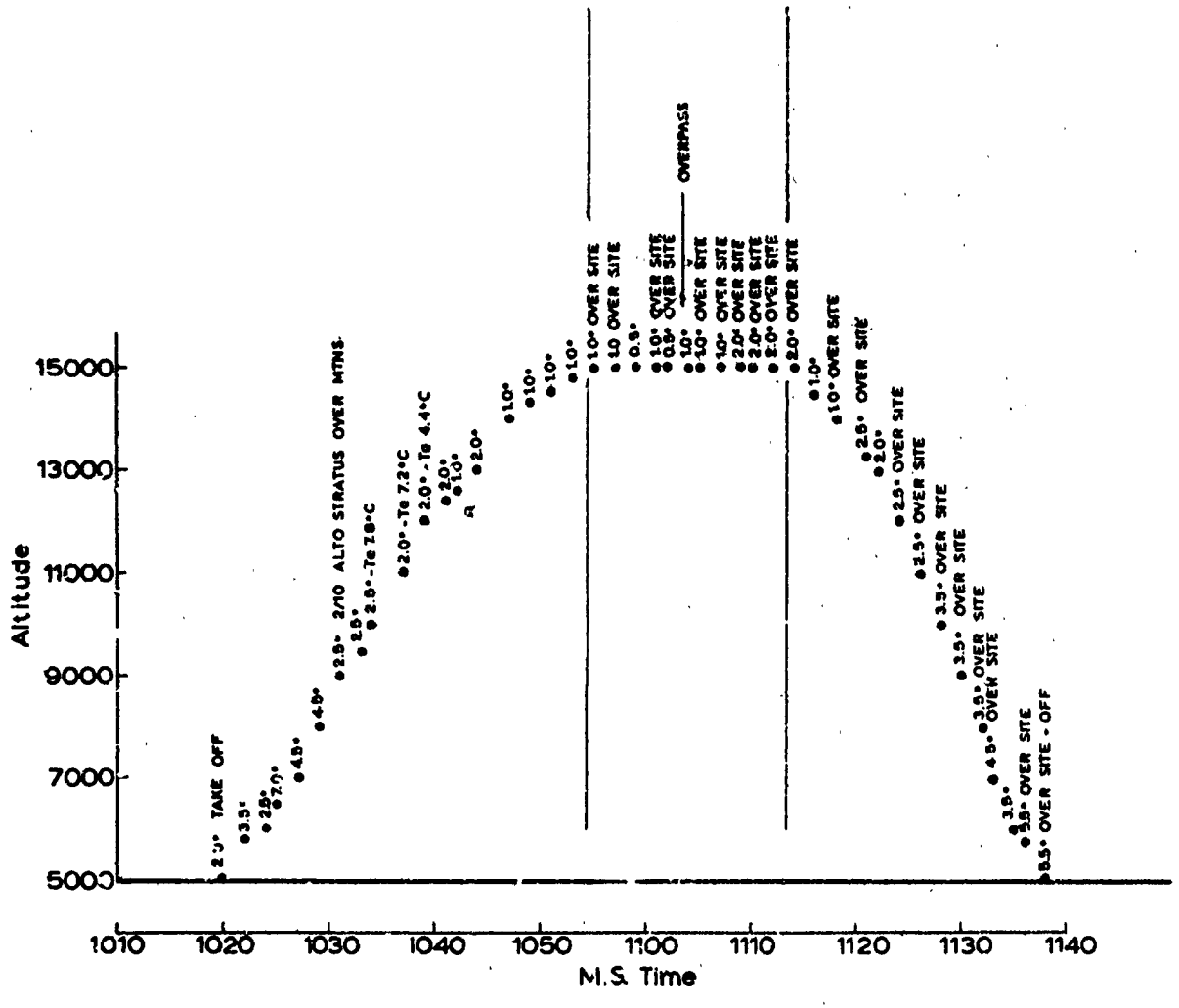

Location	Pawnee Grassland
Orbit	# 3464
Date	2-8-64
Spectrum	8—13 μ
Temp. Rad	1.3°C
Temp. Soil	10.4°C
Temp. Air	5.0°C
R.H.	58 %
Cloud Cover	.3 Ci + .1 AC OVER MOUNTAINS
Wind	Est. 50 M.P.H.-NW

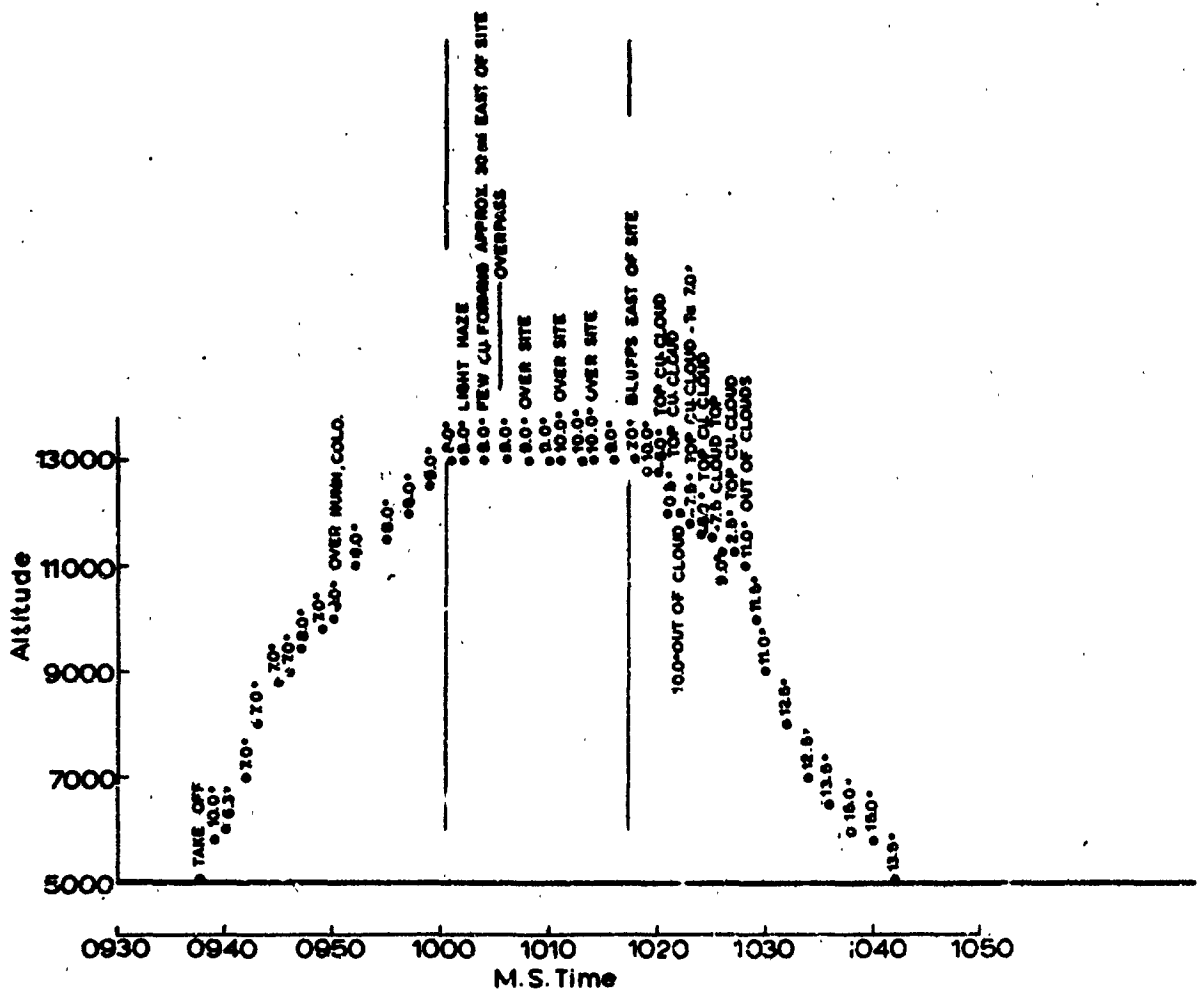

Location	Pawnee Grassland
Orbit	# 3493
Date	2-10-64
Spectrum	8-13 μ
Temp. Rad.	8.9°C
Temp. Soil	16.1°C
Temp. Air	12.7°C
R H.	86 %
Cloud Cover	FAIR WEATHER CUMULUS IN EAST OF SITE

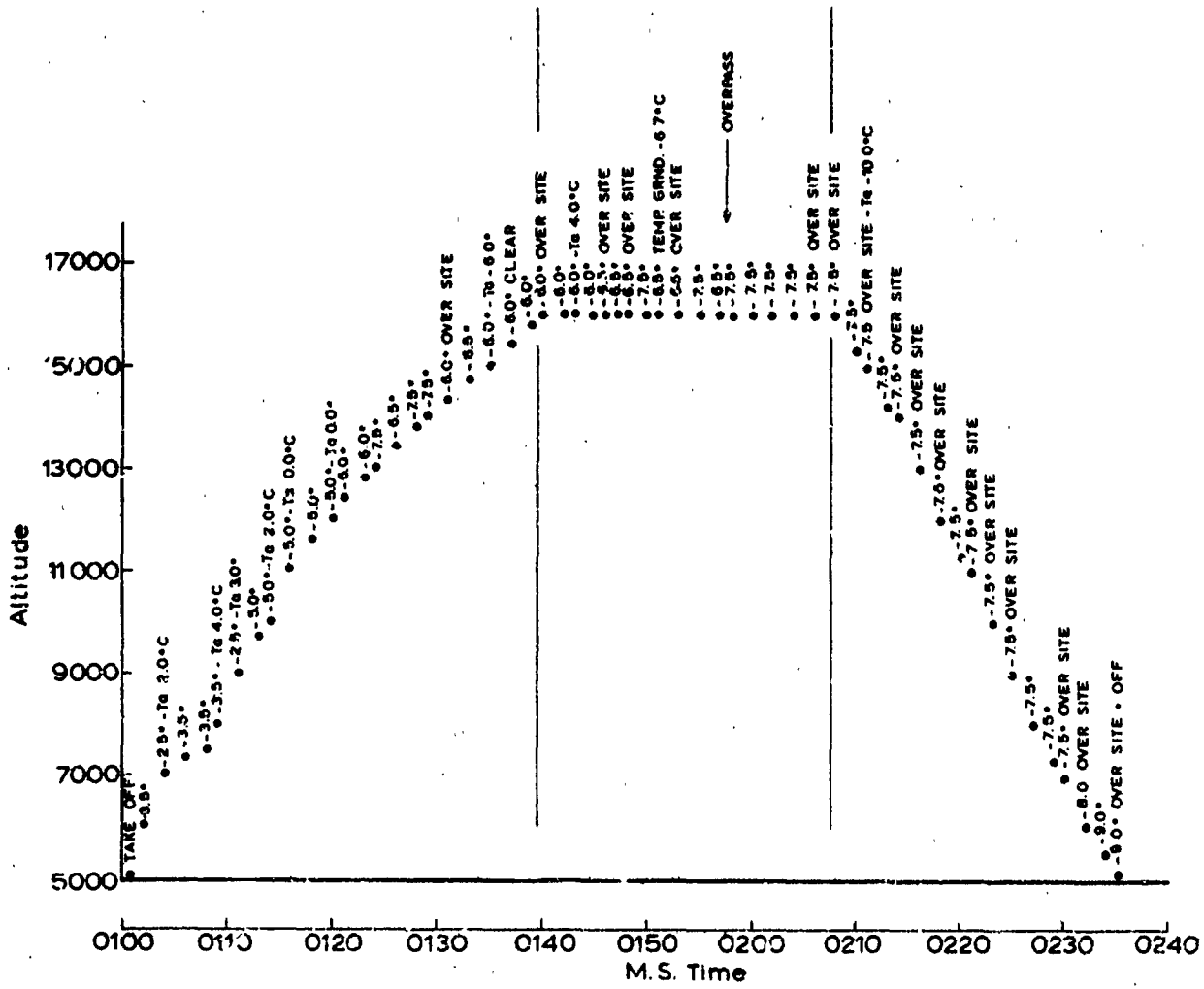

Location	Pawnee Grassland
Orbit	# 3503
Date	2-11-64
Spectrum	8-12 μ
Temp. Rad.	-6.8°C
Temp. Soil	-7.3°C
Temp. Air	-5.6°C
R.H.	Missing
Cloud Cover	Clear

Fig. 42 Minute averages of black body radiation temperatures measured over grassland from the airborne radiometers.

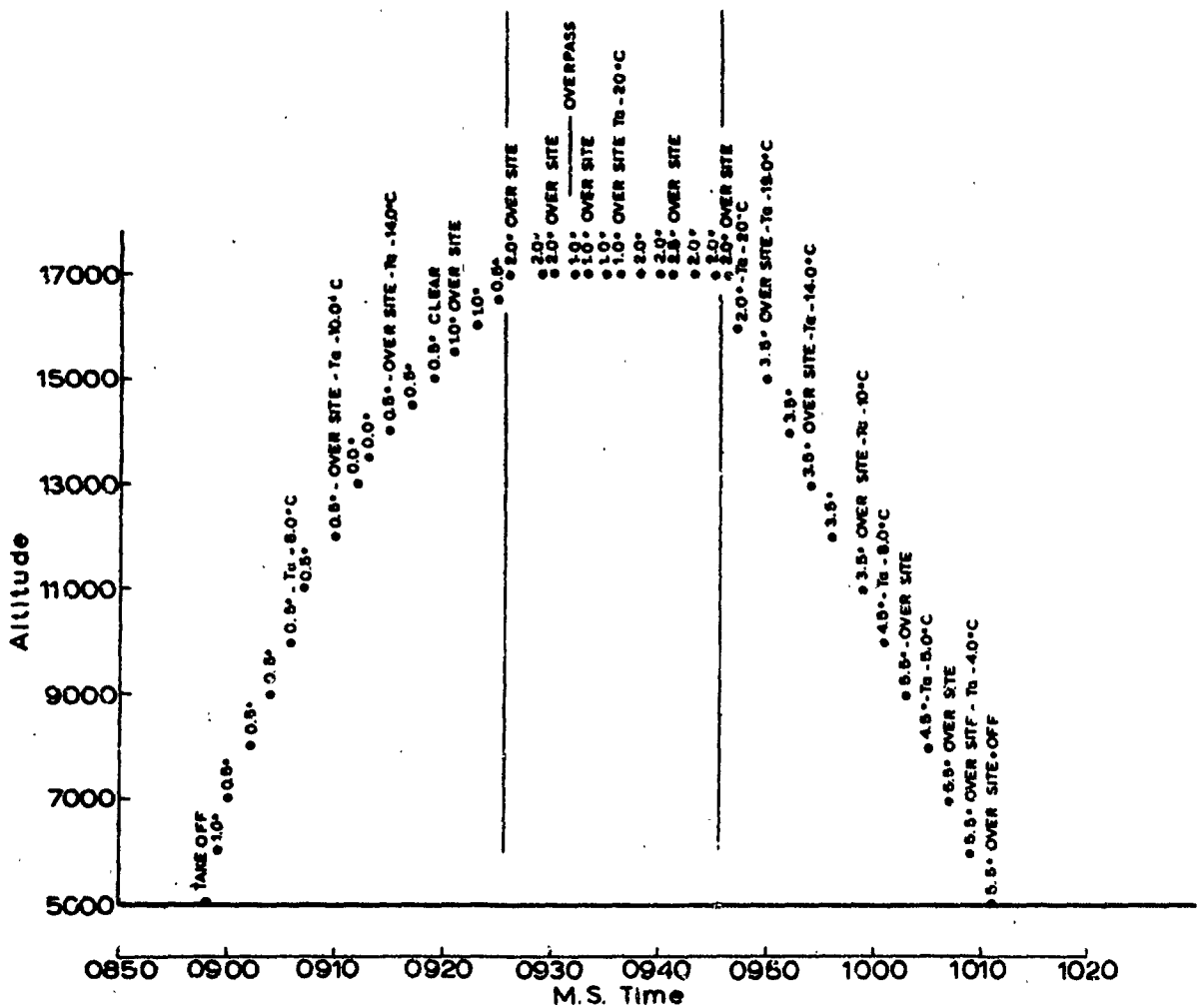

Location	Pawnee Grassland
Orbit	# 3537
Date	2-13-64
Spectrum	8-13 μ
Temp. Rad.	1.7°C
Temp. Soil	6.5°C
Temp. Air	0.6°C
R.H.	65 %
Cloud Cover	Clear

Fig. 43 Minute averages of black body radiation temperatures measured over grassland from the airborne radiometers.

OBJECTIVE II

Introduction

Under the field study of objective 2, aircraft and surface measurements were made by the Colorado State University research group in conjunction with a balloon program carried out by the Department of Astronautics and Aeronautical Engineering, University of Michigan.

The South Dakota field study was conducted to obtain measurements of terrestrial radiation at different heights in the atmosphere using various instruments carried by a small airplane and a skyhook type balloon. It was planned that measurements using these instruments would be compared to radiation measurements from TIROS VII on its first orbits across the region. TIROS VII was launched into orbit on June 16, 1963. Due to instrument failures followed by adverse weather, the balloon borne radiometer package was not launched until June 26.

Nearly continuous aircraft measurements of terrestrial radiation (8-13 micron band) were made at various altitudes under the balloon. Earth surface temperature measurements were obtained at two locations along the flight path of the balloon.

Instrumentation

The airplane used in this study was the Colorado State University Cessna 180. Two infrared radiometers (Barnes Instrument Co., Models IT-1 and IT-2) were mounted in a camera port on the underside of the fuselage of the airplane to measure the outgoing terrestrial radiation. The IT-2 radiometer was used as the primary sensor with the older, less reliable, IT-1 used as a back-up instrument. Filters in these radiometers restricted measurements to the atmospheric window region between 8 and 13 microns. View angle of each radiometer was a 30° cone. An aerial camera (Model K-24) was also mounted in the planes fuselage to take pictures of the earth's surface. Fig. 44 shows the Cessna aircraft used. An aerograph mounted under one wing was used to record pressure, temperature and relative humidity.

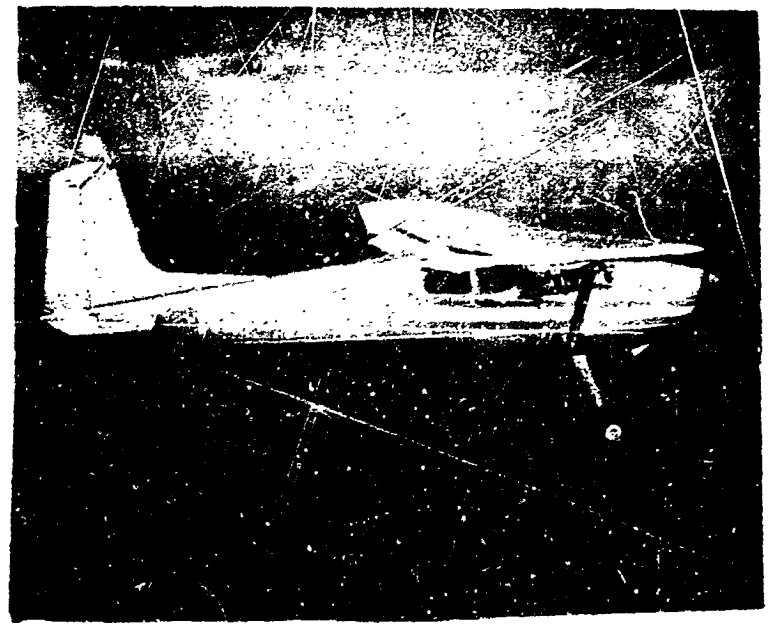

Fig. 44 Aircraft used for infrared radiation measurements.

Measurements of earth surface temperatures were obtained by a 23 point network of stabistor sensors. Accuracy of the stabistors was better than 2° F. (A more detailed description of the surface temperature equipment may be found elsewhere in this report). In addition to temperature measurements, surface soil samples were obtained for moisture content.

Site Location

The first set of surface temperature measurements were obtained approximately five miles southeast of Mitchell, South Dakota in shortgrass pasture (2-4 inches tall). Other vegetation in the area consisted of bare ground, corn fields (mostly bare), wheat and other grain.

Measurements were made at this site between 0840 and 0930 CST. During the period that these surface temperatures were being recorded, a profile of outgoing radiation was obtained from the surface to an altitude of 17,000 feet m.s.l. over the general area. The balloon, travelling almost due west at an altitude of 110,000 feet m.s.l., appeared to pass directly over the Mitchell site between 0900 and 0930.

Skies over eastern South Dakota between 0800 and 0930 CST were clear. Surface wind was southeast five knots (estimated).

The second surface temperature observation site was located approximately 7 miles south of White River, South Dakota. This site was also a grassland pasture; however, the grass was generally much taller than that at the Mitchell site. Average grass height here ranged from six to twenty-four inches. Nearly all of the vegetation in the region around White River consisted of grass pastureland. The stabistors were placed within the grass cover near the ground surface.

The surface temperature units at each location were shielded from the direct rays of the sun.

Results and Discussion

Fig. 45 shows the terrestrial radiation measurements obtained by the IT-2 radiometer aboard the aircraft. Tables 3 and 4 list the surface and radiation temperature measurements at the two sites. Table 5 summarizes the measurements made at the two sites.

A layer of broken cumulus clouds moved over the White River site during the period of measurement. Bases of these clouds were approximately 10,000 feet with tops near 13,000 feet m.s.l. The effect of cooler areas of the earth surface in the cloud shadows is noted in the comparison of radiation temperatures to surface temperatures. When the plane was above 13,000 feet m.s.l., the radiometers integrated the radiation from the cloud tops as well as the earth surface.

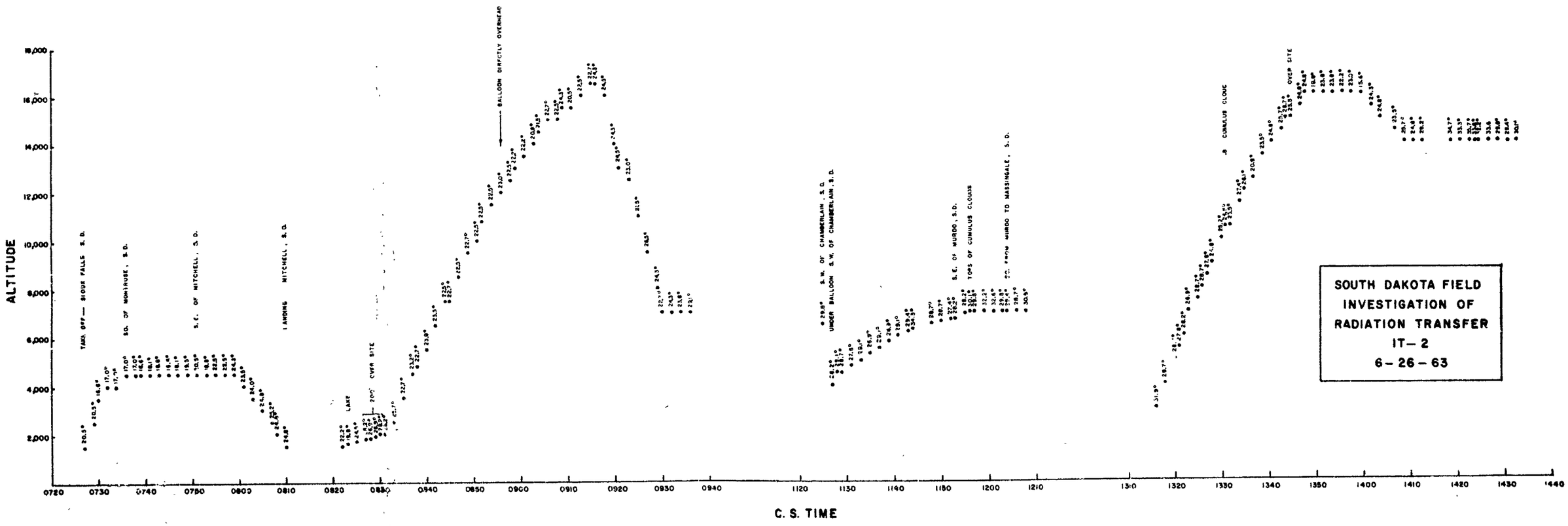

Fig 45. Radiation temperature measurements, 8-13 micron, June 26, 1963.

TABLE 3. Surface and Radiometer Temperature Measurements. Mitchell, South Dakota Site.

Time	Surface	Temp. (°C)	Altitude (m.s.l.)	Sensor
0823	Small lake	19.8	1,600	IT-2
0820	Corn field (mostly bare)	26.9	1,850	IT-2
0820	Wheat-corn complex	26.9	1,900	IT-2
0830	Pasture (over site)	28.2	1,950	IT-2
0835	Pasture (over site)	22.7	3,500	IT-2
0840	Crop-pasture complex	23.8	5,500	IT-2
0845	Crop-pasture complex	22.7	7,500	IT-2
0850	Crop-pasture complex	22.5	10,800	IT-2
0852	Crop-pasture complex	22.2	13,000	IT-2
0903	Crop-pasture complex	20.8	14,000	IT-2
0906	Crop-pasture complex	22.7	15,000	IT-2
0913	Crop-pasture complex	22.5	16,000	IT-2
0920	Crop-pasture complex	24.3	14,000	IT-2
0925	Crop-pasture complex	21.5	11,000	IT-2
0930	Crop-pasture complex	22.7	7,000	IT-2
0840-0930	Pasture	29.4	surface	Stabistor

TABLE 4. Surface and Radiometer Temperature Measurements. White River South Dakota Site.

Time	Surface	Temp. (°C)	Altitude (m. s. l.)	Sensor
1322	Pasture	28.2	6,000	IT-2
1326	Pasture	28.7	8,000	IT-2
1330	Pasture	25.2	10,000	IT-2
1333	Pasture	25.4	11,000	IT-2
1335	Pasture	26.1	12,000	IT-2
1338	Pasture	22.2	13,000	IT-2
1341	Pasture	24.8	14,000	IT-2
1330-1340	Pasture	41.0	surface	stabistor
1344	Pasture	28.7	15,000	IT-2
1345	Pasture	23.5	15,000	IT-2
1348	Pasture	24.8	16,000	IT-2
1350	Pasture	18.8	16,000	IT-2
1340-1350	Pasture	39.6	surface	stabistor
1354	Pasture	23.8	6,000	IT-2
1358	Pasture	23.0	8,000	IT-2
1400	Pasture	15.6	10,000	IT-2
1404	Pasture	24.8	15,000	IT-2
1409	Pasture	25.7	14,000	IT-2

TABLE 5. Surface and Aircraft Measurements. South Dakota Balloon and Satellite Field Study, June 26, 1963.

	Site I	Site II
Location	5 mi. SE Mitchell	7 mi. S. White River
Time	0840-0830 C.S.T.	1330-1350 C.S.T.
Radiometer temp. (°C), IT-1	20.3	18.6
Radiometer temp. (°C), IT-2	23.0	24.9
Number observations, IT-1	23	16
Number observations, IT-2	23	13
Soil surface temp. (°C)	29.4	40 40.3
Number observations	52	52
Air temp. (°C)	26.4	30.6
Relative humidity (%)	58	62
Precipitation table, H_2O (in.)	.76	1.00
Cloud cover	clear	40%
Remarks	excellent conditions	balloon above clouds

Fig. 46 shows the 8-13 micron radiation temperature measured by the TIROS channel 2 radiometer aboard the balloon gondola. Fig. 46 supplied by Dr. Hartman of the University of Michigan.

The second objective of this phase of the study will be to obtain the measurements of earth surface temperatures and radiation in the 8-13 and 9-11 micron band of the spectrum over a vegetationless desert region, a dry lake bed near Edwards Air Force Base, California. Measurements at approximately 20,000 and 45,000 feet will be compared to actual surface temperatures and to TIROS VII measurements if available.

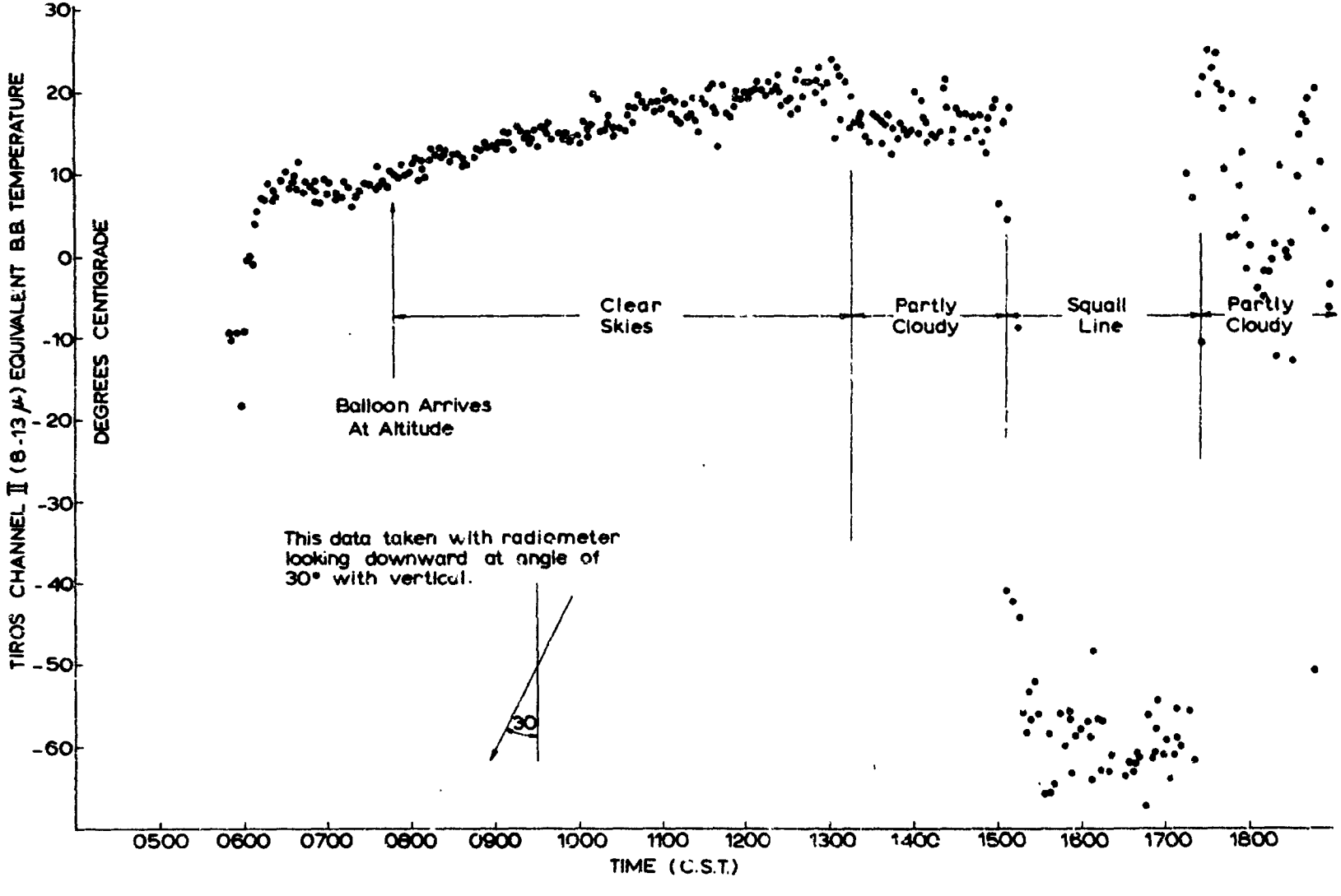
TIROS CHANNEL II (8-13 μ) EQUIVALENT B.B. TEMPERATURE
DEGREES CENTIGRADE
30
20
10
0
-10
-20
-30
-40
-50
-60
Clear Skies
Partly Cloudy
Squall Line
Partly Cloudy
Balloon Arrives At Altitude
This data taken with radiometer looking downward at angle of 30° with vertical.
30
0500
0600
0700
0800
0900
1000
1100
1200
1300
1400
1500
1600
1700
1800
TIME (C.S.T.)

OBJECTIVE III

Introduction

This objective is a study of the black body radiation temperature of cloud tops as compared to the air temperature outside the cloud at the same altitude. The optical depth of the cloud i.e. the distance into the cloud that the radiometer "sees", is dependent upon both the density and the nature of the cloud droplets. Cirriform and other thin cloud layers do not absorb all the incoming radiation. Satellite radiometers tend to overestimate the temperature of these cloud tops.

From the small amount of data collected thus far, (Table 6) it appears that the water droplets of cumulus cloud tops are several degrees colder than the air at the same altitude. The difference in temperature is probably due to the fact that the droplets at the top of the cloud are being cooled by evaporation. Measurements over an alto-cumulus cloud deck, however, showed cloud droplet temperatures somewhat warmer than the free air temperature at cloud top height.

The lack of suitable clouds, in particular, clouds with tops below 18,000 feet over the high plains of northern Colorado have limited this phase of the study. A field trip to the Gulf of Mexico region is planned for early April to study cloud radiation characteristics.

OBJECTIVE IV

The investigation of spectral emissivity characteristics of clouds and earth surfaces has been delayed until the University of Michigan personnel have completed their studies with the Perkins-Elmer spectrometer.

TABLE 6. Comparison of Cloud Radiation Temperatures to Air Temperatures (8-13 micron)

Date	Time	Altitude	Cloud Type	Black Body Temp. °C	Air Temp. °C
Location: Over site at Briggsdale, Colorado					
11/11/63	1522	18,000	Thin cirrus top	- 6.0	-12.5
	1540	18,000	Between layers at clouds	- 5.0	-13.0
	1549	15,000	Alto-cumulus top	-10.0	- 6.6
	1550	14,500	Alto-cumulus top	- 9.0	- 6.6
Location: Colorado Springs, Colorado					
12/31/63	1114	17,500	Alto-cumulus top	-10.5	-18.8
	1116	18,000	Alto-cumulus and alto-stratus deck	-15.5	-19.4
	1125	18,000	Alto-cumulus top	-17.0	-20.5
	1134	18,000	Alto-cumulus top	-17.0	-21.1

BIBLIOGRAPHY

Bandeen, W. R., R. A. Hanel, J. Licht, R. A. Stompfl, and W. G. Stroud, 1961: Infrared flux and surface temperature from the TIROS II meteorological satellite. J. Geophys. Res., 65, 3169-3185.

Brooks, F. A., 1959: Physical microclimatology. University of California, Davis, Calif., 253 pp.

Fritz, S. and J. S. Winston, 1962: Synoptic use of radiation measurements from satellite TIROS II. Mon. Wea. Rev., 90, 1-9.

Gates, David M., 1962: Energy exchange in the biosphere. Harper and Row, New York, 151 pp.

Hanel, R. A., and W. G. Stroud, 1961: The TIROS II radiation experiment. Tellus, 13, 486-488.

List, Robert J., 1951: Smithsonian Meteorological Tables. Vol. 114, Sixth Edition, Smithsonian Inst., Washington, D. C.

Moon, Parry, 1940: Proposed standard solar radiation curves for engineering use. Journal Franklin Inst., 230 (5), 583-617.

Wark, D. Q., G. Yamamoto, and J. H. Lienesch, 1962: Methods of estimating infrared flux and surface temperature from meteorological satellites. J. Atmos. Sci., 19, 369-384.

ACKNOWLEDGMENT

I wish to thank each member of the research team who have so diligently helped in the collection and analysis of the data summarized in this report.

APPENDIX A

Laboratory Investigation of Infrared Radiation and Soil Emissivity

by

Alan Anderson

Radiometer Sensitivity

A series of tests were conducted in an environmental chamber to determine the sensitivity of the Barnes Infrared Radiometer instruments.

In these tests a radiometer with a 9-11 micron filter was located in the chamber above a seven foot square area covered with about three inches of grassland topsoil. The soil used was typical of that found in Northeastern Colorado where aircraft and ground measurements are being conducted to determine surface temperatures. The sensing head of the radiometer was positioned such that its field of view included only area covered by the topsoil. Conditions in the chamber were stabilized near 25°C. and 20% relative humidity.

The actual tests involved the use of two smaller areas of the same topsoil which were superimposed upon the larger base area. One of these had an area equal to about 6% of the total area viewed by the radiometer, the other 24%.

These smaller areas were then heated or cooled so that a stabilized temperature differential $(T_a - T_b)$ existed between them and the base area. (T_a is the temperature of the small area and T_b that of the base).

After this temperature differential was established, the smaller areas were moved to various positions with respect to the center of the viewing area of the radiometer and the following measurements were recorded:

The distance from the center of the smaller area to the center of the viewing area in terms of percentage of viewing area radius was plotted as an abscissa (D).

The temperatures measured by the radiometer with the smaller areas in these various positions were recorded and converted to equivalent black body radiation values (R'). The radiometer measured temperature of the uniform base area was also converted to an equivalent black body radiation value (R_o) . The difference (R_o - R') was then converted to a percent change in R_o ; $(R_o - R')/R_o \times 100\%$ and plotted as the ordinate (ΔR_o).

The temperature differentials were created and maintained by an electrically powered nichrome wire grid for heating and dry ice under an aluminum plate for cooling.

The change in radiation due to an area of temperature differential is proportional to the magnitude and area of the differential and inversely proportion to its distance from the center of the area being viewed. Thus the area near the center of the viewing field is the most important in determining the mean temperature of the field as measured by this radiometer.

As can be seen from the accompanying figures (Figs. A. 1-9) even when a temperature differential of 13.3° C. exists over 24% of the view area, the maximum radiation change is only about 11% (Fig. A. 1).

The amount of this maximum change is, of course, still lower when the area and/or magnitude of the differential is decreased. The maximum change in radiation when a temperature differential of 13.9° C. covers 6% of the view area is only about 2% (Fig. A. 8).

The values of temperature differentials used are thought to approximate those actually occurring in the field.

Soil Emissivity

The emissivity of the grassland soil was estimated in the following way:

A portable infrared source (Model 11-140, Extended Area Infrared Radiation Source manufactured by the Barnes Engineering Company) with an emissivity of 0.92 ± 2% was put into the environmental chamber and left there so that its temperature became equal to that of the soil.

The 9-11 micron radiometer was then used to measure the emitted radiation from each surface separately. At the time of the test, the

temperatures of the emitting surfaces were 26.2°C. and 26.3°C. for the reference source and soil respectively. The outgoing radiation as measured by the 9-11 micron radiometer was the same for both surfaces.

If one allows for the error introduced by the instruments, the temperatures of the two surfaces are also equal. Thus one can conclude that the emissivity of the soil used was approximately equal to that of the reference source ($e = 0.92$).

Further emissivity tests are planned, both in the environmental chamber and in the field using an "emissivity box" similar to the one designed by the Department of Meteorology, University of Washington.

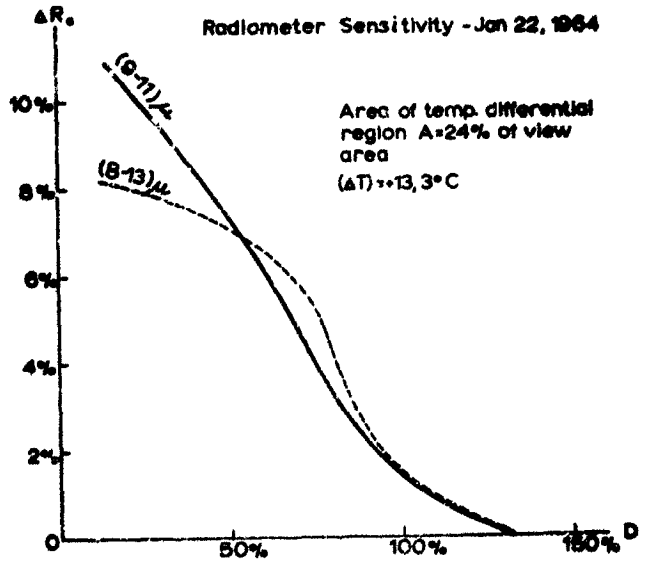

Fig. A.1 Relationship between radiometer measurement and the position of a temperature differential of given magnitude and area. $\Delta T = 13.3°C$. $A = 24\%$.

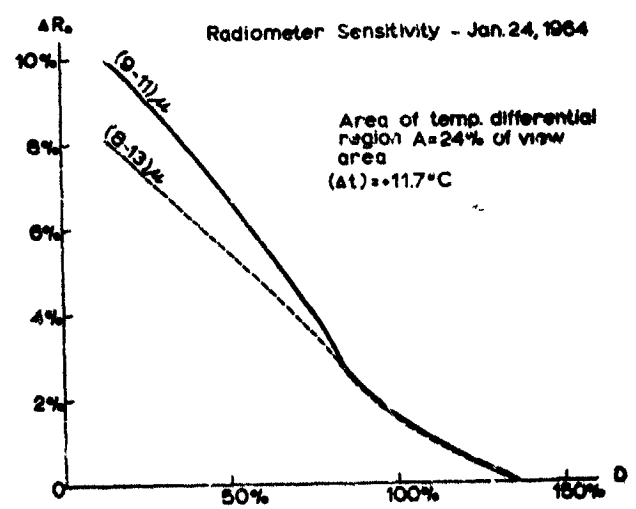

Fig. A.2 Same as Fig. A.1. $\Delta T = 11.7°C$. $A = 24\%$.

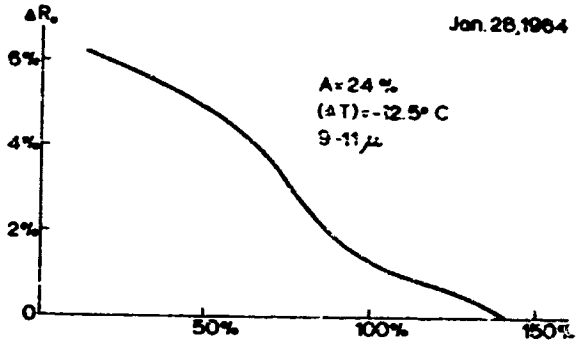

Fig. A.3 Same as Fig. A.1. $\Delta T = -12.5°C$. $A = 24\%$.

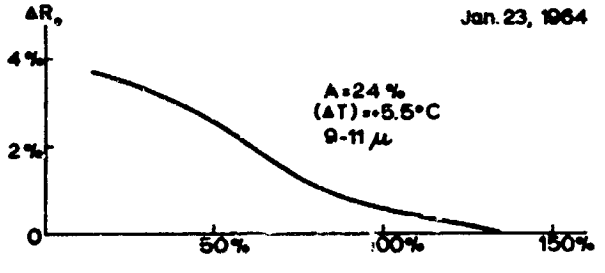

Fig. A.4 Same as Fig. A.1. $\Delta T = 5.5°C$. $A = 24\%$.

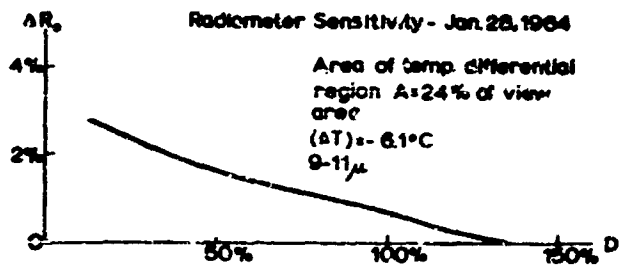

Fig. A. 5 Same as Fig. A. 1. $\Delta T = -6.1°C$. A= 24%.

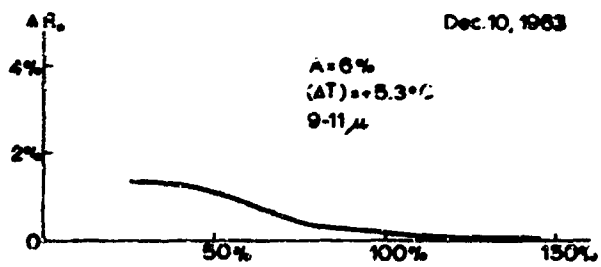

Fig. A. 6 Same as Fig. A. 1. $\Delta T = 5.3°C$. A = 6%.

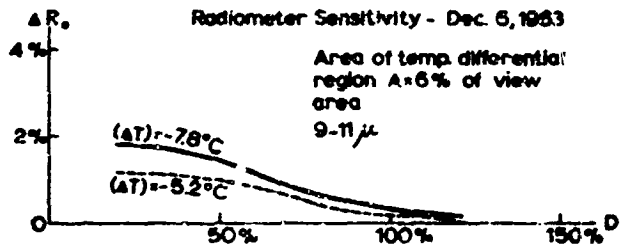

Fig. A.7 Same as Fig. A.1. $\Delta T = -7.8°C$. $\Delta T = -5.2°C$. $A = 6\%$.

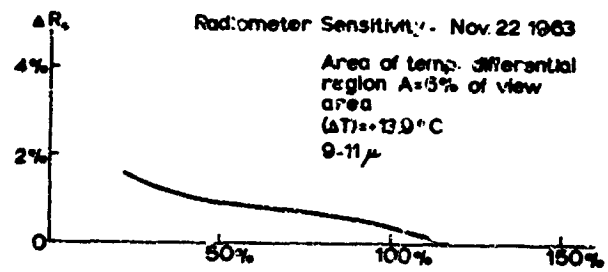

Fig. A.8 Same as Fig. A.1. $\Delta T = 13.9°C$. $A = 6\%$.

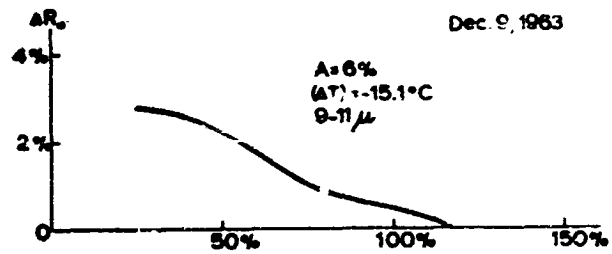

Fig. A. 9 Same as Fig. A. 1. $\Delta T = -15.1°$ C. $A = 6\%$.

APPENDIX B

An Indirect Approach for the Evaluation of the Concentration of Particulate Material in Atmospheric Haze

by

A. D. Tabler

Introduction

When aircraft measurements of outgoing terrestrial radiation in the 8-13 micron waveband were compared to actual earth surface temperatures for various synoptic conditions it was observed that the absorption of radiation by the atmosphere is related to the turbidity of the lowest layers of the atmosphere. Absorption of long wave radiation by the atmosphere for six cases when the aircraft observer reported light to dense haze averaged 11.1% greater than for an equal number of "clean" atmosphere cases.

The effect of atmospheric haze on incoming solar radiation was also measured. A number of flights were made with an Eppley pyrheliometer mounted on the top of the airplane (Fig. B.1). Measurements with this instrument were recorded simultaneously with another Eppley pyrheliometer at the surface. From comparison of these measurements (Figs. B.2, 3, 4) one can get an estimate of the absorption of solar radiation by haze layers.

Objective

To test the feasibility of this approach to the quantitative evaluation of the density of atmospheric haze, an experiment was conducted to determine the dust content of the lower air over Fort Collins, Colorado using the Brooks(1959) equation for transmittance of whole spectrum direct beam solar radiation.

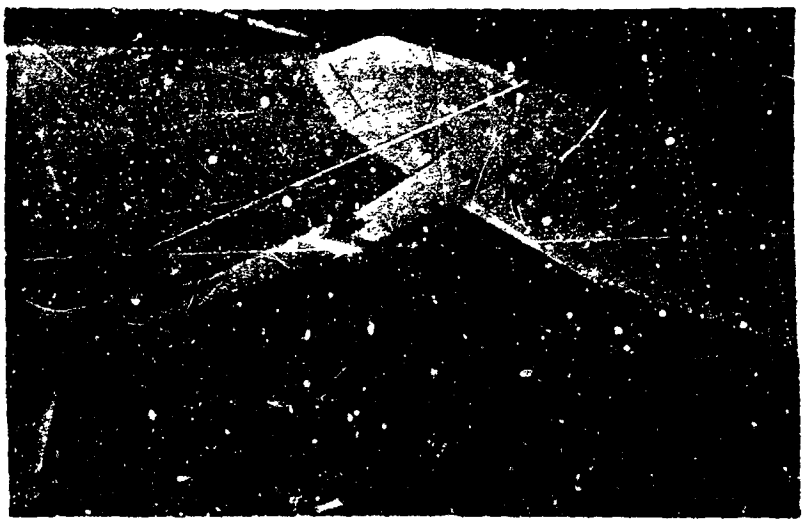

Fig. B. 1 Eppley pyrheliometer mounted on top of the aircraft for measurement of incoming solar radiation.

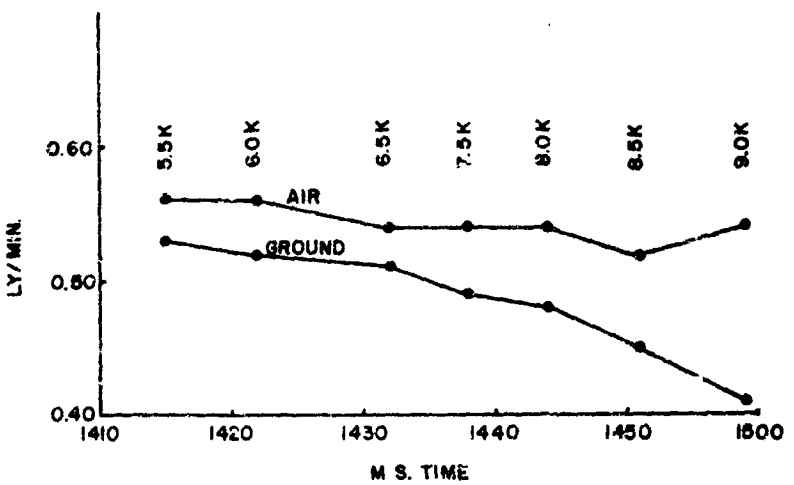

Fig. B. 2 Simultaneous measurements of incoming solar radiation from Eppley pyrheliometers on the ground and on the top of the Cessna 180. November 1, 1964.

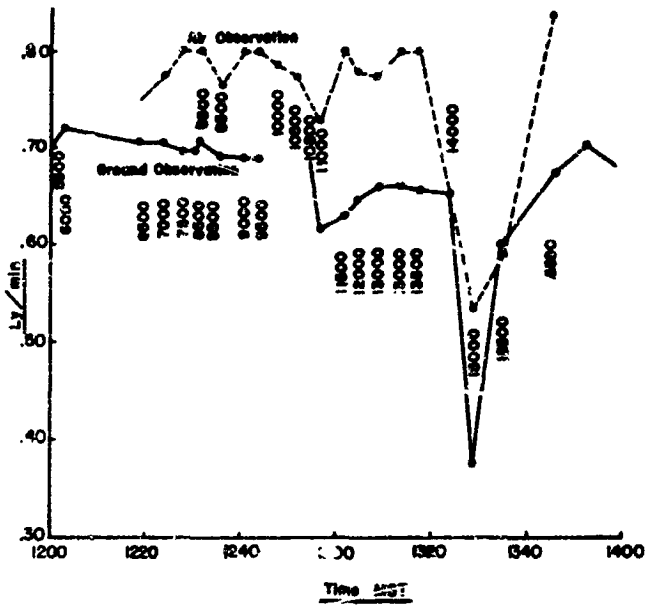

Fig. B. 3 Simultaneous measurements of incoming sol radiation from Eppley pyrheliometers on the ground and on the top of the Cessna 180. January 21, 1964.

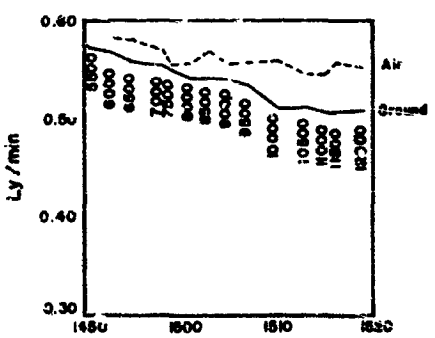

Fig. B. 4 Same as Fig. B. 3. February 10, 1964.

Procedure

On November 13, 1963 between about 1500 and 1600 MST, simultaneous solar radiation measurements were made with an Eppley pyrheliometer on the ground and another mounted on a Cessna aircraft. These measurements were repeated with the aircraft at 500 feet elevation levels starting at an elevation of 5,500 feet and continuing to 8,000 feet m.s.l. Elevation angles of the sun were recorded for each measurement. Pressure and air temperature measurements also were taken from the aircraft. A Denver radiosonde sounding (1700 MST) was obtained from which precipitable water was computed for the levels of interest after verifying the similarity of the Denver observations with the aircraft temperature and pressure data.

The basic Brooks' equation (1959) as modified by Gates (1962) is as follows:

$$Q_p = \frac{2.0}{r^2} \exp\left[-0.089\,(PM/1013)^{0.75} - 0.174\,(WM/20)^{0.6} - 0.83\,(dM)^{0.9} \right]$$

where Q_p = flux of direct sunlight on a surface perpendicular to the sun's rays in ly/min.
p = air pressure in mb.
w = total precipitable water vapor in the atmosphere in the zenith direction (in min.)
d = concentration of dust particles in number/cc
m = air mass
r = radius vector of the earth

The above equation was modified to allow computations based on differences between ground and air measurements to be used rather than the absolute values of ground and aircraft incident radiation. This adaptation seemed desirable for several reasons. First, recorded values of radiation were higher than should have been obtained due principally to the small elevation angle of the sun (Fig. B.5). Conversion of horizontal radiation measurements to values of sunlight received on a surface normal to the sun's rays is accomplished by multiplying the recorded readings by the cosecant of of the sun's elevation angle. Since csc' $\alpha \rightarrow \infty$ $\alpha \rightarrow 0°$ elevation angles must be measured very precisely if errors are to be kept within acceptable limits. This source of error could be minimized by working with differences between ground and aircraft measurements. A second reason for modifying the equation was to obviate the need for precipitable water measurements throughout the total atmosphere. Thirdly, since the basic

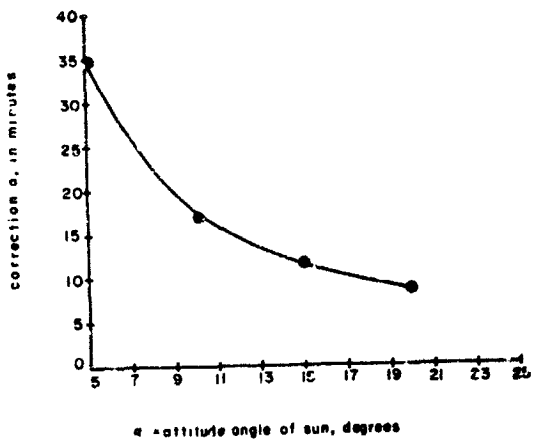

Fig. B. 5 Graphical correction of pyrheliometer measurements of incoming radiation for changes in sun angle.

equation has been derived for direct sunlight radiation, the influence of scattered and diffuse radiation on the final results is kept to a minimum. It should be emphasized that the modification of the equation for layer analysis is required only when the error effects noted above are of such a magnitude as to result in negative values of the exponential term when applied individually to ground or aircraft readings. If positive values of the exponent were obtained, subtracting the calculated dust concentration based on the ground reading from that based on the aircraft observation would eliminate the error sources noted above as well as the modified differential layer form of the equation. In this experiment preliminary analysis indicated that development of the following equations was essential.

The theory of the modification is that the nature of the depletion function is the same for a small differential layer of air as it is for the total atmosphere. Since the original Brooks equation is empirical, the validity of the foregoing assumption would have to be tested experimentally. The utility of this approach should justify future research with this intent.

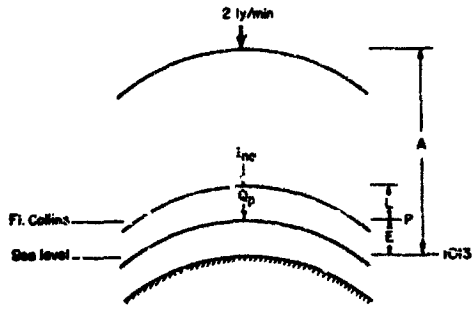

Derivation of equation:

Let I_{na} = normal incident direct beam radiation at the top of the layer L in question. This value is analogous to and replaces T_2/r^2 of the original equation (ly/min).

L = the thickness of the air layer of interest, whose lower boundary coincides with the ground surface at some elevation E above m. s. l. (ft.).

P = total pressure at the ground at the bottom of L . This is the same term as in Brooks' equation (mb).

Q_p = normal incident direct-beam solar radiation at ground level at the bottom of L . This is the same term as in Brooks' equation (ly/min).

ΔP_m = the differential pressure of the air layer L , as measured by the aircraft (mb).

ΔP_s = the theoretical differential pressure of the air layer L for the standard atmosphere (mb).

ΔW_m = measured precipitable water content of the layer L (in mm).

ΔW_s = theoretical precipitable water content of the layer L for the standard atmosphere (in mm).

The air depletion term of the Brooks equation, $0.089(MP/1013)^{0.75}$ relates atmospheric pressure to the number of air molecules which are available for absorption and scattering of solar radiation in the total atmosphere above the point where Q_p is measured. The term $P/1013$ includes two corrections, one of which is for air mass characteristics at the time of observation. For the air layer L, by analogy, $\Delta P_m/\Delta P_s$ corrects for air mass characteristics, and elevational differences are not involved due to the differential treatment. The number of air molecules involved in depletion must now be reduced for the layer by the ratio L/A. This can be accomplished utilizing the pressure terms $\Delta P_m/P$ so as to obviate the need for density correction. The modified air molecule depletion term now becomes

$$0.089\left[\left(\frac{M\Delta P_m}{\Delta P_s}\right)\left(\frac{\Delta P_m}{P}\right)\right]^{.75} = 0.089\left[\frac{M\overline{\Delta P}_m^{\,2}}{P\Delta P_s}\right]^{.75}$$

The air mass term M is unchanged due to its definition.

Directly analogous reasoning results in the differential water molecule depletion term

$$0.174\left[\left(\frac{M\Delta W_m}{\Delta W_s}\right)\left(\frac{\Delta P_m}{P}\right)\right]^{0.6}$$

The portion of this expression $\frac{\Delta P_m}{P}$ reducing the effective depth of the atmosphere assumes that the water vapor is distributed in the atmosphere in the same fashion as are the air molecules. It must be emphasized that this is only an approximation and could be in error under certain conditions.

The resultant differential layer form of the transmittance equation may now be written

$$Q_p = I_{na}\exp\left[-0.089\left(\frac{M\overline{\Delta P}_m^{\,2}}{P\Delta P_s}\right)^{0.75} - 0.174\left(\frac{M\Delta W_m\Delta P_m}{P\Delta W_s}\right)^{0.6} - 0.083(dM)^{0.9}\right]$$

solving in terms of d,

$$d = \frac{1}{m}\left[\frac{\ln I_{na} - 0.089\left(\frac{M\overline{\Delta P}_m^{\,2}}{P\Delta P_s}\right)^{0.75} - 0.174\left(\frac{M\Delta W_m\Delta P_m}{P\Delta W_s}\right)^{0.6} - \ln Q_p}{0.083}\right]$$

The susceptibility of the results to errors in calculating M is still present in the final equation, and is the largest potential source of

error at low sun angles. To minimize this error, a more refined form of estimating M was used in this experiment rather than assuming $M = \csc \beta$ (where β = elevation angle of the sun). For the purposes of this experiment, $M = \csc (\beta + C)$ where C = correction factor denoting the departure of $\csc \beta$ from the optical air mass. Values of C were calculated from Table 137 of the Smithsonian Meteorological Tables (1951).

Results

1. Observations corresponding to aircraft elevations of 6,500 feet were discarded because the C_p observations at the ground were larger than those at the plane. Remaining data yielded the following results:

Layer ft.	Ave. dust conc. particles/cc	Relative dust conc. particles/cc/ft.
sfc. - 5500	0	0
5500 - 6000	0.846	0.001694
6000 - 7000	1.787	0.001787
7000 - 7500	0	0
7500 - 8000	0	0

Elev. level ft.	Cumulative dust concentration particles/cc
sfc - 5500	0
sfc - 6000	0.510
sfc - 7000	1.21
sfc - 7500	0.942
sf - 8000	0.777

Figs. B.6 and B.7 show the results graphically.

2. The orders of magnitude of the results are reasonable.

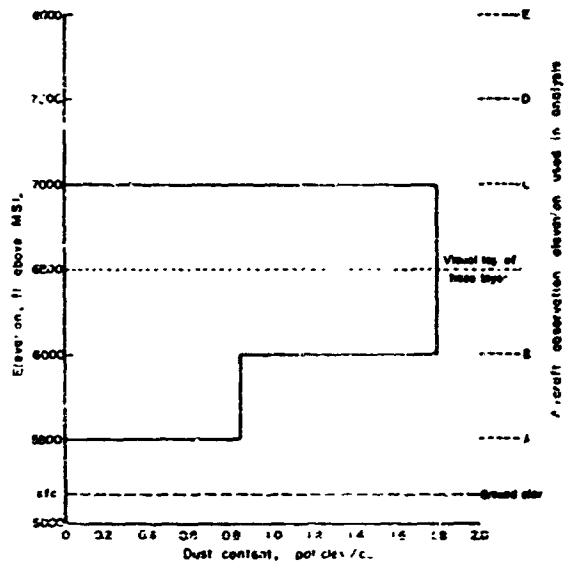

Fig. B.6 Average dust and haze content of the lower atmosphere above Fort Collins, Colorado, 1300 MST, November 13, 1963.

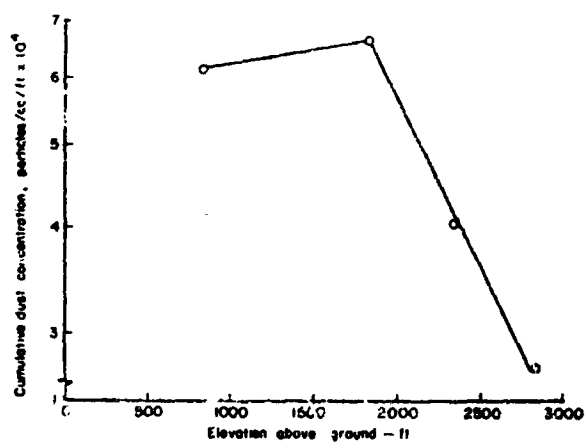

Fig. B.7 Change in relative dust concentration with elevation at Fort Collins, Colorado, 1300 MST, November 13, 1963.

3. The calculated upper limit of the dust concentration (3000-7000 ft.) corresponds well to the visual top of the haze layer observed during the experiment (3500 ft.)

4. The change in calculated cumulative dust concentration with height above 7000 feet agrees almost perfectly with the theoretical values assuming negligible dust content above 7000 feet.

5. The principal discrepancy in the results appears to be the absence of dust in the surface - 5500 foot layer.

Sources of error: The primary source of error using the modified equation is that introduced in the calculation of the optical air mass M ; the low sun angles prevailing during the experiment probably account for a major part of the discrepancies in the results.

Standard Atmosphere Constants

Elev. ft.	Elev. m.	ΔP_s mb.	$\bar{w}$ g/kg	P_w mm	P mb.	w g/kg	Accum. ΔP_s mb.	Accum. P_w mm.
5170(sfc)	1580				837.4	6.3	0	0
5500	1680	10.1	6.25	0.644	827.3	6.2	10.1	0.644
6000	1830	15.2	6.00	0.930	812.1	5.8	25.3	1.574
6500	1980	15.2	5.7[illegible]	0.884	796.9	5.6	40.5	2.458
7000	2140	15.5	5.42	0.858	781.4	5.25	56.0	3.316
7500	2280	13.5	5.12	0.705	767.9	5.0	69.5	4.021
8000	2440	15.3	4.9	0.765	752.6	4.8	84.8	4.786
8500	2590	14.0	4.65	0.664	738.6	4.5	97.8	5.450
9000	2740	13.8	4.38	0.618	724.8	4.25	112.6	6.066

Tabulation of Data and Calculated Values

Elev. ft.	Sun L deg.	CSC Sun L	Ground Data			Aircraft Data			Aircraft Air temp. °F	Aircraft		Denver Raob pressure mb.
			M. V.	Ly/min.	I_n	M. V.	Ly/min.	I_n		Pressure in.	Pressure mb.	
5170									47.2	24.71	837	844.5
5500	13.5	4.284	0.87	0.34[illegible]	1.49	3.4	0.354	1.52	46.2	24.43	828	835.1
6000	13.0	4.445	0.79	0.316	1.40	3.8	0.396	1.76	45.2	23.98	810	820.8
6500	12.3	4.694	0.90	0.360	1.69	3.72	0.357	1.67	45.0	23.53	796	806.5
7000	11.8	4.890	0.51	0.204	1.00	3.15	0.328	1.60	53.5	23.09	782	792.2
7500	11.3	5.103	0.31	0.124	0.633	1.87	0.195	0.995	54.0	27.65	757	777.9
8000	10.7	5.386	0.27	0.108	0.581	1.58	0.1645	0.891	53.8	22.22	754	763.6
8500	10.3	5.595	0.36	0.144	0.805	1.50	0.1561	0.873	52.3	21.80	738	749.3
9000	9.7	5.835	0.43	0.172	1.02	1.46	0.152	0.900	51.2	21.385	690	735.0

Elev. ft.	Denver Raob R.H. (%)	Raob mixing ratio g/kg	Raob precipitable water (in)	"a" min.	α + a deg. + min.	m = csc (α + a)	Raob precipitable water (mm)	Aircraft ΔP accum. mb.
5170		4.0						
5500	46	3.3	0.0138	12	13-42	4.222	0.350	9
6000	42	3.1	0.0184	13	13-13	4.374	0.467	27
6500	46	3.5	0.0189	14	12-32	4.608	0.470	
7000	32	3.0	0.0186	14	12- 2	4.797	0.472	
7500	17	1.9	0.0140	15	11-33	4.994	0.357	
8000	17	1.85	0.0107	16	10-58	5.257	0.274	
8500	16	1.75	0.0103	17	10-35	5.445	0.262	99
9000	16	1.70	0.0099	17	9-59	5.768	0.252	

Calculations:

1. Calculations of precipitable water from Denver Raob:

$$P_w = 1/980 \int_{P_1}^{P_2} W \, dp$$

where P_w = precipitable water in cm.
W = mixing ratio in g/kg.
dp = pressure change in millibars.

a. 5170 - 5500 ft.

$P_w = 1/980\ (3.65)\ (844.5 - 835.1)$
$= 3.65/980\ (9.4) = 3.50 \times 10^{-2}$ cm
$= 0.350$ mm (0.0138 in.)

b. 5500-6000 ft.

$P_w = 3.2/980\ (835.1 - 820.8)$
$= 3.2/980\ (14.3) = 4.67 \times 10^{-2}$ cm
$= 0.467$ mm (.0184 in.)

c. 6000 - 6500 ft.

$P_w = 3.3/980\ (820.8 - 806.5)$
$= 3.3/980\ (14.3) = 4.81 \times 10^{-2}$ cm
$= 0.481$ mm (0.189 in.)

d. 6500 - 7000 ft.

$P_w = 3.25/980\ (806.5 - 792.2)$
$= 3.25/980\ (14.3) = 4.75 \times 10^{-2}$ cm
$= 0.475$ mm

e. 7000 - 7500 ft.

$P_w = 2.45/980\ (792.2 - 777.9)$
$= 2.45/980\ (14.3) = 3.58 \times 10^{-2}$ cm
$= 0.358$ mm

f. 7500 - 8000 ft.

$$P_w = 1.875/980\ (777.9 - 763.6)$$
$$= 1.875/980\ (14.3) = 2.74 \times 10^{-2}\ \text{cm}$$
$$= 0.274\ \text{mm}$$

g. 8000 - 8500 ft.

$$P_w = 1.80/980\ (763.6 - 749.3)$$
$$= 1.80/980\ (14.3) = 2.63 \times 10^{-2}\ \text{cm}$$
$$= 0.263\ \text{mm}$$

h. 8500 - 9000 ft.

$$P_w = 1.725/980\ (749.3 - 735.0)$$
$$= 1.725/980\ (14.3) = 2.52 \times 10^{-2}\ \text{cm}$$
$$= 0.252\ \text{mm}$$

2. Calculation of dust concentrations surface to 5500.

I_{na} = 1.52 ly/min

ΔP_m = 9.0 mb

ΔP_s = 10.1 mb

M = 4.222

ΔW_M = 0.35 mm

ΔW_s = 0.644 mm

Q_p = 1.49 ly/min

Calculation of factors:

1. $\ln I_{na} = l_n\ 1.52 = 0.41871$

2. $$\left(\frac{\Delta P_m M}{\Delta P_s}\right)\left(\frac{\Delta P_m}{P_B}\right) = \frac{(9)\ (4.222)\ (9.0)}{(10.1)\quad(837)} = 0.0405$$

3. $(0.0405)^{.75} = 0.0905$

4. $\left(\frac{\Delta W_m M}{\Delta W_s}\right)\left(\frac{\Delta P_m}{P_B}\right) = \frac{(0.35)(4.222)(9.0)}{(0.644)(837)} = 0.0247$

5. $(0.0247)^{0.6} = 0.1088$

6. $\ln Q_p = \ln 1.49 = 0.3988$

substitute in equation:

$$d = \frac{1}{4.222}\left[\frac{0.41871 - 0.089(0.0905) - 0.174(0.1088) - 0.3988}{0.083}\right]^{1.11}$$

$$= \frac{1}{4.222}\left[\frac{0.41871 - 0.00805 - 0.01891 - 0.3988}{0.083}\right]^{1.11}$$

$$= \frac{1}{4.222}\left(\frac{-.00705}{0.083}\right)^{1.11} = \frac{1}{4.22}\left(-0.085\right)^{1.11}$$

$\therefore d = 0$ w/in. limits of experiment error ← surface to 5500 ft.

Surface to 6000 ft.

$I_{na} = 1.76$ ly/min
$\Delta P_m = 27$ mb
$\Delta P_s = 25.3$ mb
$m = 4.374$
$\Delta W_m = 0.817$
$\Delta W_s = 1.574$
$Q_p = 1.40$ ly/min.

Calculation of factors:

1. $\ln I_{na} = \ln 1.76 = 0.56531$

2. $\left(\frac{\Delta P_m M}{\Delta P_s}\right)\left(\frac{\Delta P_m}{P_B}\right) = \frac{(27)(4.374)(27)}{(25.3)(837)} = 0.1504$

3. $(0.1504)^{0.75} = 0.242$

4. $\left(\frac{\Delta W_m M}{\Delta W_s}\right)\left(\frac{\Delta P_m}{P_B}\right) = \frac{(0.817)(4.374)(27)}{(1.574)(837)} = 0.0731$

5. $(.0731)^{.6} = 0.208$

6. $\ln Q_p = \ln 1.40 = 0.33647$

substitute in equation:

$$d = \frac{1}{m}\left[\frac{0.56531 - 0.089(.242) - 0.174(0.208) - 0.33647}{0.083}\right]^{1.11}$$

$$= \frac{1}{m}\left[\frac{0.56531 - 0.02153 - 0.0362 - 0.33647}{0.083}\right]^{1.11}$$

$$= \frac{1}{4.374}\left(\frac{0.17111}{0.083}\right)^{1.11} = \frac{1}{4.374}(2.06)^{1.11}$$

$$= \frac{1}{4.374}(2.23) = 0.51$$

$\therefore d = 0.510$ particles/cc ← surface to 6000 ft.

Surface to 7000 ft.

$I_{na} = 1.60$ ly/min.
$\Delta P_m = 55$ mb
$\Delta P_s = 56$ mb
$m = 4.797$
$\Delta W_m = 1.759$
$\Delta W_s = 3.316$
$Q_p = 1.00$ ly/min.

Calculation of factors:

1. $\left(\frac{\Delta P_m M}{\Delta P_s}\right)\left(\frac{\Delta P_m}{P_B}\right) = \frac{(55)(4.797)(55)}{(56)(837)} = 0.309$

2. $(0.309)^{0.75} = 0.415$

3. $\ln I_{na} = \ln 1.60 = 0.47000$

4. $\left(\frac{\Delta W_m M}{\Delta W_s}\right)\left(\frac{\Delta P_m}{P_B}\right) = \frac{(1.759)(4.797)(55)}{(3.316)\quad(837)} = 0.167$

5. $(0.167)^{0.6} = 0.342$

6. $\ln Q_p = \ln 1.00 = 0$

substitute in equation:

$$d = \frac{1}{4.797}\left[\frac{0.47000 - 0.089(0.415) - 0.174(0.1672)}{0.083}\right]^{1.11}$$

$$= \frac{1}{4.797}\left[\frac{0.47000 - 0.0369 - 0.0291}{0.083}\right]^{1.11}$$

$$= \frac{1}{4.797}\left(\frac{0.404}{0.083}\right)^{1.11} = \frac{1}{4.797}(4.87)^{1.11} = \frac{5.79}{4.797}$$

$\therefore d = 1.21$ particles/cc ← surface to 7000 ft.

Surface to 7500 ft.

$I_{na} = 0.995$ ly/min
$\Delta P_m = 70$ mb
$\Delta P_s = 69.5$ mb
$m = 4.994$
$\Delta W_m = 2.116$ mm
$\Delta W_s = 4.021$ mm
$Q_p = 0.633$ ly/min.

Calculation of factors:

1. $\ln I_{na} = \ln 0.995 = -0.005$

2. $\left(\frac{\Delta P_m M}{\Delta P_s}\right)\left(\frac{\Delta P_m}{P_B}\right) = \frac{(70)(4.994)(70)}{(69.5)(837} = 0.420$

3. $(0.42)^{0.75} = 0.524$

4. $\left(\frac{\Delta WM}{\Delta W_s}\right)\left(\frac{\Delta P_m}{P_B}\right) = \frac{(2.116)(4\ 994)(70)}{(4.021)(837)} = 0.219$

5. $(0.219)^{0.6} = 0.402$

6. $\ln Q_p = \ln 0.633 = -0.457$

substitute in equation:

$$d = \frac{1}{4.994}\left[\frac{-0.005 - 0.089(0.524) - 0.174(0.402) + 0.457}{0.083}\right]^{1.11}$$

$$= \frac{1}{4.994}\left[\frac{-0.005 - 0.0465 - 0.0700 + 0.457}{0.083}\right]^{1.11}$$

$$= \frac{1}{4.994}\left(\frac{0.3355}{0.083}\right)^{1.11} = \frac{1}{4.994}(4.04)^{1.11} = \frac{4.70}{4.994}$$

$\therefore d = 0.942$ particles/cc ← surface to 7500 ft.

Surface to 8000 ft.

$I_{na} = 0.891$ ly/min
$\Delta P_m = 83$ mb
$\Delta P_s = 83.8$ mb
$m = 5.257$
$\Delta W_M = 2.390$ mm
$\Delta W_s = 4.786$ mm
$Q_p = 0.581$ ly/min.

Calculation of factors:

1. $\ln I_{na} = \ln 0.891 = -0.11541$

2. $\left(\frac{\Delta P_m M}{\Delta P_s}\right) \left(\frac{\Delta P_m}{P_B}\right) = \frac{(8.3)(5.257)(83)}{(83.8)(837)} = 0.516$

3. $(0.516)^{0.75} = 0.611$

4. $\left(\frac{\Delta W_m M}{\Delta W_s}\right) \left(\frac{\Delta P_m}{P_B}\right) = \frac{(2.39)(5.257)(83)}{(4.786)(837)} = 0.261$

5. $(0.261)^{0.6} = 0.446$

6. $\ln Q_p = \ln 0.581 = -0.543$

substitute in equation:

$$d = \frac{1}{5.257} \left[\frac{-0.11541 - 0.089(0.611) - 0.174(0.446) + 0.543}{0.083}\right]^{1.11}$$

$$= \frac{1}{5.257} \left[\frac{-0.11541 - 0.0544 - 0.0775 + 0.543}{0.083}\right]^{1.11}$$

$$= \frac{1}{5.257} \left(\frac{0.2957}{0.083}\right)^{1.11} = \frac{1}{5.257} (3.56)^{1.11} = \frac{4.09}{5.257}$$

$\therefore d = 0.777$ particles/cc ← surface to 8000 ft.

3. Conversion of concentrations in layers from ground to aircraft to concentrations in elevational zones.

1. Concentration in layer surface to 5500 ft. (5170 - 5500 ft.)

$C = 0$ particles/cc ← surface to 5500 ft.

2. 5500 - 6000 ft.

$$\frac{(330)(0) + (500)(X)}{830} = 0.51 \text{ particles/cc}$$

$$\therefore \frac{500X}{830} = 0.51$$

$$X = \frac{(0.51)(830)}{500} = 0.846 \text{ particles/cc}$$

$\therefore C = 0.846$ particles/cc ← 5500-6000 ft.

3. 6000 - 7000 ft.

$$\frac{(330)(0) + (500)(0.846) + (1000)(X)}{1830} = 1.21 \text{ particles/cc}$$

$$\therefore 423 + 1000X = 2210$$

$$\therefore X = \frac{2210 - 423}{1000} = \frac{1787}{1000} = 1.787 \text{ particles/cc}$$

$$\therefore C = 1.787 \text{ particles/cc} \longleftarrow \text{6000 - 7000 ft.}$$

4. 7000 - 7500 ft.

$$\frac{(330)(0) + (500)(0.846) + (1000)(1.787) + (500)(X)}{2330} = 0.942 \text{ part./cc}$$

$$423 = 1787 + 500X = 2195$$

$$\therefore X = \frac{2195 - 423 - 1787}{500} = \frac{-15}{500} = 0.0$$

$$\therefore C = 0 \text{ particles/cc} \longleftarrow \text{7000 - 7500 ft.}$$

5. 7500 - 8000 ft.

$$\frac{(330)(0) + (500)(.846) + (1000)(1.787) + (500)(0) + (500)(X)}{2830} = 0.777$$

$$\therefore 423 + 1787 + 500X = (2830)(0.777)$$

$$\therefore X = \frac{2200 - 2210}{500} = \frac{-10}{500}$$

$$\therefore C = 0.0 \text{ particles/cc} \longleftarrow \text{7500 - 8000 ft.}$$

Conclusions

This experiment shows that it is possible to obtain a quantitative evaluation of the concentration of particles in atmospheric hazes. There are, however, several criticisms of this method. First, the basic equation by Brocks, based on observations and calculations by Moon (1940) is empirical. It is difficult or impossible to evaluate the accuracy of the constants used in the equation. Second, haze density may not have the same effect on terrestrial radiation that it has on solar radiation. Third, the density of haze layers varies with the wind speed and temperature lapse rates in the atmosphere. Measurements made at one time of the day may not be meaningful a few hours later.

Further investigation of this approach to evaluation of haze density is planned.